Energy Conversion and Management: X 12 (2021) 100110

Contents lists available at ScienceDirect

Energy Conversion and Management: X

journal homepage: www.sciencedirect.com/journal/energy-conversion-and-management-x

Energy flexible CHP-DHN systems: Unlocking the flexibility in a real plant

A. Mugnini [a,*], G. Comodi [a], D. Salvi [a,b], A. Arteconi [a,c]

[a] Dipartimento di Ingegneria Industriale Scienze Matematiche, Università Politecnica delle Marche, via Brecce Bianche, 1, 60131 Ancona, Italy
[b] Astea Spa, Osimo, AN, Italy
[c] Department of Mechanical Engineering, KU Leuven, B-3000 Leuven, Belgium

ARTICLE INFO

Keywords:
Energy flexibility
Cogeneration
District heating network
Thermal energy storage

ABSTRACT

The purpose of this paper is to identify and analyze the impact of flexibility enablers in cogeneration and district heating network (CHP-DHN) plants by means of a real case study located in central Italy. A wider definition of energy flexibility applicable to the entire energy supply chain (i.e. production, transport and usage) is used in this analysis. In particular the flexibility is intended as the capability of each part of the system to produce a variation in its load curve, while ensuring the required performance. In this sense energy efficiency technologies, the use of energy storage and advanced control techniques can be seen as flexibility enablers potentially available in each section of the energy system.

The innovative contribution of this work is to propose flexibility strategies in compliance with the constraints imposed by both the managers and users. The study aims to show possible ways to activate flexibility services to be used with known instruments and to quantify their impact with a simulation-based approach. In particular, three different flexibility instruments are identified in different sections of the plant: (i) the use of a thermal energy storage (TES) in the generation side, (ii) the optimal management of the DHN supply temperature (energy distribution side) and (iii) the management of the thermostatically controlled loads (TCLs) of the final users (demand side) connected to the network. Through the implementation of simulation models calibrated with available measurements, the influence of these flexibility instruments on the energy/environmental performance is evaluated in comparison to the current configuration of the plant. Results confirm the great impact of the TES to increase the CHP working hours and, as a consequence, a primary energy saving increase is obtained in mid-season and in summer season. Whereas the optimal management of the water supply temperature in the DHN allows to obtain 1% fuel reduction in a typical winter week and 2% in a typical summer week. As far as the activation of the demand side flexibility is concerned, the effect of the management of TCLs on energy conservation is demonstrated: 1 °C reduction of the setpoint of all the residential users during a typical winter day produces a 7.3% reduction of the DHN thermal demand. However, its impact on the generation side (i.e. to reduce the electricity/thermal production of the CHP at specific times) is limited due to the characteristics of the considered CHP plant (the CHP engine is sized to cover only the thermal baseload and it scarcely affected by thermal demand variations). The analysis proposed helps to obtain valuable hints on unlocking the energy flexibility in CHP-DHN plants useful for a better management of such systems.

1. Introduction

The European Union, with the presentation of the new Green Deal policy program [1], has drawn up a roadmap to become the first climate-neutral continent by 2050. From the objectives it proposes, it is easy to deduce that ensuring the balance between supply and demand while minimizing the resulting environmental impact is one of the main challenges posed by the clean energy transition. Indeed, the maximization of the integration of renewable energy sources will make necessary the promotion of policies aimed at increasing the flexibility of the whole energy system. As the International Renewable Energy Agency (IRENA) also suggests, to effectively manage large-scale variable renewable energy, sources of flexibility need to be identified across all sectors of the energy system, from power generation to transmission and distribution systems, storage and demand [2].

About the latter point, the actions aimed at modifying the energy demand to adapt it to the supply are known as Demand Side Management (DSM) [3]. A DSM strategy can be applied to achieve several

* Corresponding author.
E-mail address: a.mugnini@univpm.it (A. Mugnini).

https://doi.org/10.1016/j.ecmx.2021.100110
Received 23 June 2021; Received in revised form 31 August 2021; Accepted 15 September 2021
Available online 21 September 2021

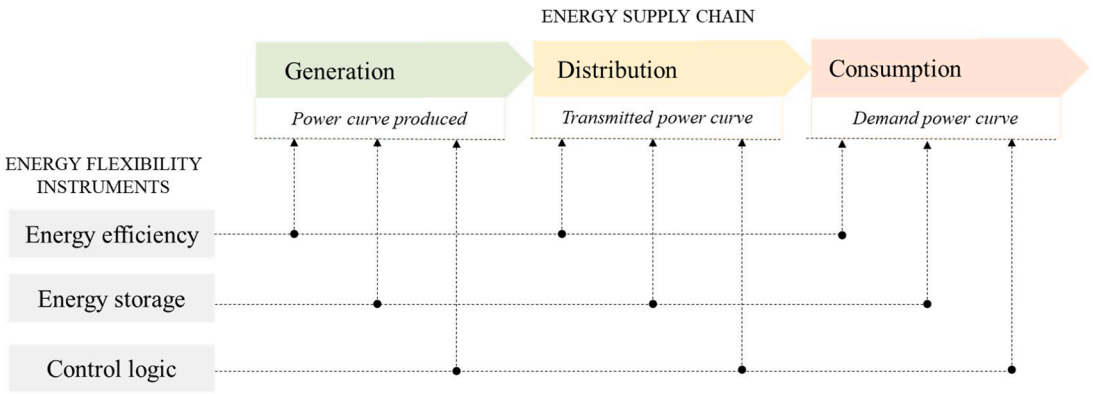

Fig. 1. Schematic of the energy flexibility in a complete energy system.

objectives to increase the flexibility of the system, such as peak shaving, valley filling, load shifting, energy conservation, and strategic load growth [4]. Taking up in turn the work proposed by Gellings [4], Arteconi and Polonara [5] have classified in three main categories the possible technologies to produce a strategy of DSM: (i) energy-efficient devices; (ii) energy storage and (iii) communication systems between end-users and external parties (i.e, demand response strategies). If the adoption of energy efficiency devices can only produce strategies for energy conservation, the use of energy storage systems and/or demand response strategies can be used to vary punctually and programmed the final user's demand curve.

The classification provided by Arteconi and Polonara [5] is designed for the activation of the energy flexibility in buildings. However, such definition of energy flexibility could also be extended to larger-scale systems, which includes the entire energy chain (i.e. from production to consumption and transport). In general terms, being flexible can be understood as the ability of a system to adapt to different situations, while ensuring the required performance. In an energy system, the definition can be translated as a measure of the ability to modify and/or manage its load curves. Consequently, the three categories of flexibility enablers introduced in [5] can be introduced also for energy systems. In particular, considering the entire energy chain, the flexibility can be activated for different purposes by means of: (i) energy efficiency measures, (ii) the use of an energy storage system and (iii) the implementation of advanced control logics. Once again, energy efficiency measures (i) produce flexibility services from the prospective of the energy conservation. In a wider context the fuel saving obtained because of the intervention could be properly managed for specific objectives or produce flexibility services when the generation system requiring more than one energy carrier is introduced (i.e., power-to heat systems). On the other hand, energy storage systems (ii) permit to decouple the energy demand from the generation and therefore to adapt the power supply curve in function of a management strategy. Finally, the use of advanced control techniques (iii) can be understood as an adaptation of the concept of demand response in buildings to the case of the energy system, since it allows to obtain punctual variations of the load and/or of the demand curves in relation to an objective to be pursued or to an external incentive.

All three flexibility enablers can be referred separately to each section of the energy system (generation, distribution and demand side, Fig. 1) and encouraged by different objectives (i.e. energy savings, optimal management of different energy carriers, economic benefits or integration of intermittent renewable energy sources) which provide benefits for system operators and/or users.

Considering the above definition, in this paper a flexibility analysis on a real case study is presented. It is composed of an Integrated Combined Heat and Power plants (CHPs) combined with a District Heating Networks (DHNs) to meet the thermal demands of a small town in the Central Italy (Osimo, 43°29′ N, 13°29′ E).

Besides being a real case study, of which measured data are available, this energy system is also interesting from the point of view of the specific technologies studied. Indeed, DHNs are considered by the European regulatory authorities as the main technologies to increase the global efficiency and the flexibility of the space heating sector due to the fact that different generation systems can be combined with them [6]. In fact, DHNs can integrate renewable energy sources [7], waste energy [89], heat pumps technologies [10] and cogeneration plants [11]. This latter technology attracts also considerable interest from the European regulation authority which suggests to encourage the dissemination of high-efficiency cogeneration and district heating networks (CHP-DHNs) to obtain high primary energy savings [12].

Several works are available in literature that highlight the ability of the different parts of CHP-DHNs plants to produce power load variations, although in some cases they are not identified as flexibility assessments. Using the definition of energy flexibility provided above and introducing the classification of the energy flexibility enablers (i.e. efficiency, storage and control) applied to the different sections of the considered energy system (i.e. generation, distribution and demand), it is possible to group accordingly the papers available in the literature and some examples are reported and discussed in the following paragraphs.

Staring form the generation side, Zhang et al. [13] proposed a novel cogeneration system equipped with organic Rankine cycle and an absorption heat pump to recover condensate waste heat of exhaust steam from the steam turbine in a direct air-cooling coal-fired power plant. In this study is presented as an energy and exergy analysis and the obtained results show total energy and exergy efficiency increases of 11.97% and 4.01% respectively. From a system perspective, the solution proposed in the study is aimed to produce reductions in the consumption curve of the generation side at unchanged performance, so it can be seen as a flexibility enabler that produce an energy conservation strategy. The same applies to the use of a thermal storage system with an optimal control technique in the study proposed by Bogdan and Kopjar [14]. In this paper, the authors evaluated the economical and the environmental benefits that the addition of a Thermal Energy Storage (TES) to a cogeneration plant allows to achieve. Referring to a real system located in Zagreb (Croatia), the study showed that by charging the TES during the daytime when the electricity price is high, and by releasing district heat during cheap night hours, it is possible to obtain savings of about 1.8 mil Euro/year and reductions of CO_2 emission by 6.4% and SOx by 16.9%. Indeed, during the day it increases the convenience of producing electricity with CHP, while during the night, the TES is able to satisfy the demand. Again, the inclusion of the TES modifies the load curves, therefore can be intended as a flexibility enabler as well. Focusing instead on the control strategy, Shao et al. [15] investigated the flexibility that can be derived from the control of CHP generators in thermal networks with the availability of renewable sources. The authors developed an optimization model for dispatching CHP plants to minimize overall cost, while satisfying the end-users need. With the results of

this study the authors obtained a 5% reduction in operation cost when the operating flexibility is used to achieve the optimal coordination of CHP plants with renewable sources. Remaining on the generation side another interesting work is proposed by Lepiksaar et al. [16]. Through a model realized in EnergyPRO, different scenarios to increase the flexibility of a CHP serving the DHN in Tallin (Estonia) are proposed by the authors. In particular, the addition of power to heat systems and TES on the generation side in order to minimize the fluctuations of the CHP thermal load and exploit electricity from RES is evaluated. The results of this analysis showed the capability of a 150000 m^3 TES coupled with a 40 MW electric boiler to stabilise the system when power consumption is low and to reduce the Natural Gas (NG) consumption and the heat rejection respectively by 36% and 38%.

Moving to analysing the distribution section, i.e. the thermal networks, there are different papers that examinate the energy flexibility potential of a district/cooling network. In particular, Vandermeulen et al. [17] wrote a review paper addressing the topic of the energy flexibility unlocking in district heating and cooling networks. Highlighting the importance of a suitable control strategy, in this paper the authors distinguished three sources of flexibility in such systems linked to different storage levels available in the network: the thermal inertia of buildings, the use of storage units and the network itself. However, the definition of energy flexibility that Vandermeulen et al. used considers only the ability of the system to decouple the demand from the generation. With the same energy flexibility concept also Guelpa and Verda [18] reviewed the DSM techniques in DHNs. Guelpa and Verda analyzed all those works that investigate strategies to produce thermal demand modification in district heating, extending the concept of DSM, often applied to electricity demand, to the management of thermal networks. Confirming the considerations of Vandermeulen et al. [17], Guelpa and Verda identified three sources of thermal inertia that can be used for DSM purposes: (i) heat buffers installed near the generation plants or in strategic areas of the network, (ii) the water mass within the network pipelines and (iii) the building envelope.

In this regard, a very interesting work is the one proposed by Egging-Bratseth et al. [19]. The authors developed a stochastic model to minimize the total operational cost of DHNs located in Trondheim (Norway) with local waste heat utilization, seasonal storage and uncertain demand. In this study the author evaluated several scenarios taking into account the uncertainty in space heating demand. One of the most significant results from the point of view of the potential flexibility reserve concerns the use of seasonal storage in DSM purposes. In particular Egging-Bratseth et al. obtained about 37% reduction in carbon dioxide emissions, 29% generation reduction in peak hours and 10% lower operational costs. Also Ruševljuk et al. [20] have demonstrated the ability to produce variations in the energy demand curve by acting on the DHN. Indeed, the authors presented an optimized logic to increase the efficiency of a CHP connected to a DHN located in Narva (Estonia) by acting on the supply temperature and mass flow control. With the study, the authors showed that it is possible to obtain primary energy saving of about 10,000 MWh per year with a consequent increase in the efficiency of the CHP of 1.5%.

However, according to the energy flexibility definition provided in this paper, many other means could be seen as flexibility sources in DHNs. For instance, the paper presented by Dalla Rosa and Svendsen [21] aimed at evaluating the potential of energy-efficient and cost-effective solutions (e.g. flexible pre-insulated twin pipes with symmetrical or asymmetrical insulation, double pipes, and triple pipes) for DHNs in low-heat density areas. With the results of this study Dalla Rosa and Svendsen demonstrated that the asymmetrical insulation of twin pipes can lower heat loss on the supply pipe (from −4% to −8%) and practically reduce to zero the heat loss on the return pipe. Since the identification of this technological improvement leads to a decrease of the lost thermal power curve, it can be also considered as a measure that provides flexibility always with a view to energy conservation strategies. In the same manner, also the paper proposed by Sun at al. [22] can be included in a context of flexibility analysis. Indeed, Sun at al. evaluated the benefit of installing absorption heat exchangers in district heating system based on natural gas-fired (Beijing, China) to increase the primary energy efficiency. The results of the analysis showed that primary energy efficiency and heat transmission capacity of the primary heating network can be increased by about 11% and 47% respectively. Similar considerations can be made for the consumption/demand side. Papers such as that proposed by Chen et al. [23] who provided an overview of the internal and external influencing factors on energy efficiency design of buildings can also be seen as energy flexibility enablers on the demand side. At the same time all those works that evaluate the potential of planned demand shifting strategies must be included. This is the case in which the energy flexibility derives from the ability to programmatically decouple the demand from the generation or from the management of the Thermostatically Controlled Loads (TCLs). With regard to the first point, in literature several solutions have been investigated to manage buildings thermal demand [24]: the thermal mass embedded in the building envelope can be used as an energy storage [25 26] or a dedicated TES can be added to the heating/cooling system of building [27 28]. Regarding the management of TCLs, different works highlighting its impact on the energy flexibility performance are available. An example is represented by the paper proposed by Essa [29]. In this study Essa demonstrated that an home energy management programmed to adapt power consumption and generation of TCLs and photovoltaic-battery systems reduces the energy consumption by 30% while maintaining. customer's comfort. Another interesting study was also conducted in this regard by Véliz et al. [30]. The authors analyzed the effect of different flexible operational modes for thermostatically controlled appliances in off-grid smart homes composed of small renewable generations and a backup generator based on fossil fuel. The results of this study highlighted that the optimal management of TCLs in the thermal-based appliances allows to reduce by 15% the operation of the backup generator resulting in fuel savings. In both the cited studies, the ability to produce variations in the load curve (and therefore flexibility services) of single buildings is demonstrated. Another interesting work that demonstrates this ability in a residential building connected to a thermal network is the one carried out by Coccia et al. [31]. In this study the authors considered as case study a single building whose cooling requirement can be met with different sources including a district cooling network and an air to water heat pump. In particular, the electricity required by the heat pump can be produced either with photovoltaic panels installed on site or taken from the grid. The results of the study of Coccia et al. demonstrated that whit an advanced control technique (a model predictive control), able both to choose the most convenient energy source and to exploit the flexibility from TCLs, it is possible to reduce the electricity absorbed from the grid up to −71% with respect to a reference case with a rule-based control.

The analysis of the papers presented above gives an idea of the multiple possibilities of unlocking flexibility in energy systems producing specific load variations. However, often the works refer to the study of single strategies/technologies and attention is not given to the operational aspect whit the constraints and limitations that a real system has to comply with. Indeed, referring to real energy systems already operating on a large scale, the activation of flexibility instruments may not be easy because of the several technological constraints and limitations imposed by both operators and users. In fact, in most cases, the operators plan actions or variations in the management strategy to achieve greater economic benefits not directly related with the flexibility of the system. A solution can be the planning of interventions or management strategies that can increase the flexibility of the system in compliance with the requirements that the operation requires.

The objective of this paper is to present a flexibility analysis on a CHP-DHN plant currently in operation in which, compatibly with the operational constraints, different types of flexibility enablers are identified and evaluated in different sections of the plant (production, distribution, demand). The analysis is based on the extension to energy

systems of the definition of flexibility provided by Arteconi and Polonara [5] for buildings. The flexibility instruments have been identified in compliance with the technological constraints and limitations imposed by both users and the plant operator and their effectiveness have been discussed and compared. Therefore, the study can be seen as a feasibility study on possible sources of flexibility that can be identified in a real plant.

The analysis has been performed by means of a real case study. Due to the operational constraints of the system, it was not possible to identify in the case study all the possible flexibility enablers shown in Fig. 1. However, it was possible to identify a source of flexibility in each part of the plant and to evaluate their impact on the system performance in comparison with the current plant configuration. The final objective of such flexibility exploitation is the optimal management of the system by improving its energy/environmental performance.

Although the considerations and the results obtained are related to the specific case presented, they provide a useful reference to draw some suggestions and guidelines for other similar plants where unlocking the flexibility could improve the overall performance of the system in compliance with the limitations imposed by operational constraints.

2. Methods

The CHP-DHN plant under consideration in this work is a demo plant within the EU MUSEGRIDS project. In this section an analysis of possible energy flexibility strategies to improve the performance of the system was performed to assess the effectiveness of plant modifications planned within the project. Taking into account the constraints of the current plant configuration, a flexibility enabler for each section of the system was identified. They are: (i) a TES added to the generation side, (ii) the optimal management of the DHN supply temperatures for the energy distribution system and (iii) the exploitation of the energy flexibility of the final users' thermal demand through the management of their TCLs. Each of them aims at improving the energy/environmental performance of the system.

In order to evaluate the impact of new plant configurations or operating mode, simulations models were developed and validated with experimental data (data for the whole year 2018 were considered). In relation to available measurements, the simulation model follows a mixed approach: some parts (e.g., CHP and boilers) are modeled according to a black box model while other parts (e.g., DHN) are modeled with a white box approach. More details are reported in the description of the simulation model in Section 4, after detailing the case study in Section 3.

The current configuration in terms of control logic and technologies installed is used as reference scenario for comparison.

In the following subsections a description of each flexibility instrument is reported. In particular, for each of them, both the purpose of the flexibility activation and the related performance evaluation method are discussed.

2.1. Generation-side flexibility enabler

As highlighted by Bogdan and Kopjar [14], the introduction of a TES in a cogeneration plant can have a paramount role to increase the thermal efficiency and the economy of the system. The addition of a TES allows to obtain a certain decoupling between the demand and the generation that can be exploited as provider of energy flexibility for the CHP.

In this work, it is investigated the flexibility provided by the introduction of a hot water tank on the CHP circuit [32]. In particular the impact of a control strategy aimed at increasing the operational hours of the CHP is tested in comparison to the reference scenario. The idea is that the TES could be used to allow the CHP to operate for a longer time at its maximum capacity, avoiding continuous switching on/off cycles and high load modulation of the CHP. To assess the impact of this solution, the improvement in the Primary Energy Saving (PES) is evaluated:

$$\mathrm{PES} = 1 - \frac{1}{\frac{\eta_{\mathrm{th,chp}}}{\eta_{\mathrm{th,ref}}} + \frac{\eta_{\mathrm{el,chp}}}{\eta_{\mathrm{el,ref}}}} \tag{1}$$

where $\eta_{\mathrm{th,chp}}$ and $\eta_{\mathrm{el,chp}}$ are the thermal and the electrical efficiency of the CHP, while $\eta_{\mathrm{th,ref}}$ and $\eta_{\mathrm{el,ref}}$ represent the reference thermal efficiency and electric efficiency for the separate production from the same fuel.

2.2. Distribution-side flexibility enabler

Implementing optimized system management strategies can play a fundamental role in CHP-DHN plants when the primary energy use wants to be minimized. A possible action to be implemented concerns the optimal management of the DHN supply temperature to maintain the temperature in the pipelines as low as possible and avoid energy waste. In this sense, the CHP manager could decide the day ahead, based on weather forecasts, the optimal supply temperature to be provided to the DHN to satisfy the thermal demand, while minimizing the thermal losses.

To evaluate the potential primary energy savings an optimization problem is defined. It is important to note that, as described in Section 3, in the CHP-DHN plant considered in this work the primary energy minimization coincides with the minimization of the fuel consumption as the system uses a single fuel. The optimization problem is formulated to assess the optimal water supply temperatures to the DHN in order to minimize the amount of fuel used ($\mathrm{V_{NG}}$)in a considered period. The DHN supply temperature ($T_{\mathrm{sup,dhn}}$)is the decision variable of the problem. To stress the network with wide and continuous temperature variations, the supply temperature is varied on a daily basis.

The optimization problem can be formulated as:

$$\text{minimize}\left[\mathrm{V_{NG}}\left(T_{\mathrm{sup,dhn}}\right)\right] \tag{2}$$

Subject to the following constraints and boundary conditions for the decision variables:

- The final users' thermal demand ($\dot{Q}_{\mathrm{u,tot}}$)needs to be thoroughly satisfied for each timestep *k*:

$$\forall k \;\; \dot{Q}_{\mathrm{dhn}}(k) \geq \dot{Q}_{\mathrm{u,tot}}(k) \tag{3}$$

Where $\dot{Q}_{\mathrm{dhn}}$ is the total thermal demand covered by the generation side.

- The DHN flowrate ($\dot{m}_{\mathrm{dhn}}$) has to be lower than the maximum value allowed by to the pump specifications ($\dot{\mathrm{m}}_{\mathrm{dhn,max}}$):

$$\forall k \;\; \dot{m}_{\mathrm{dhn}}(k) \leq \dot{\mathrm{m}}_{\mathrm{dhn,max}} \tag{4}$$

- The water supply temperature $T_{\mathrm{sup,dhn}}$ can take values in the range between $\mathrm{T_{sup,dhn,min}}$ (fixed at 70 °C to avoid legionella issues) and a maximum value ($\mathrm{T_{sup,dhn,max}}$) for each day (*d*) of simulation:

$$\forall d \;\; \mathrm{T_{sup,dhn,min}} \leq T_{\mathrm{sup,dhn}}(d) \leq \mathrm{T_{sup,dhn,max}} \tag{5}$$

- The DHN return temperature $T_{\mathrm{ret,dhn}}$ must remain above a certain minimum ($\mathrm{T_{ret,dhn,min}}$) value to avoid excessive cooling of the network:

$$\forall k \;\; T_{\mathrm{ret,dhn}}(k) \geq \mathrm{T_{ret,dhn,min}} \tag{6}$$

The optimization is implemented in Python by means of the algorithm SLSQP (Sequential Least Squares Programming) [33]. To evaluate the potential fuel saving obtained, the results are compared to the reference scenario that represent the current operation of the plant (Section 3).

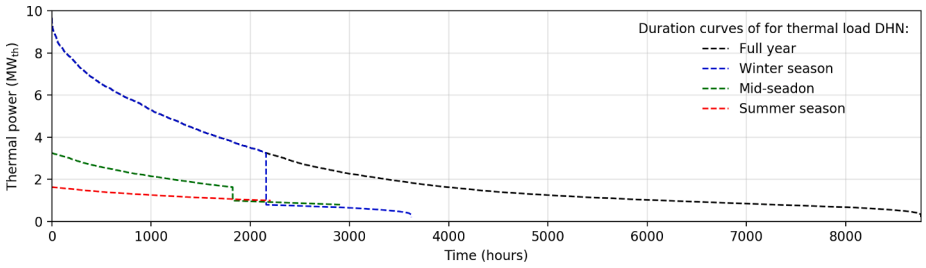

Fig. 2. Thermal load duration curve of DHN for full year (2018), winter, mid-season, and summer months.

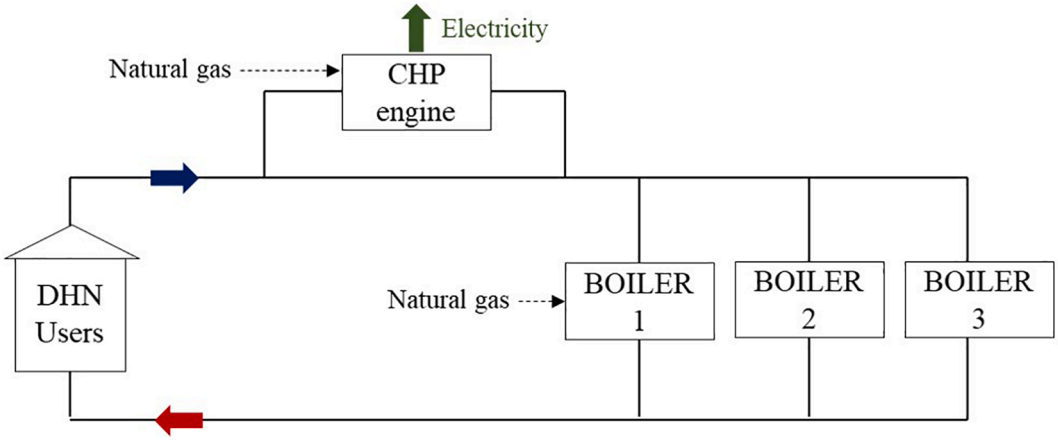

Fig. 3. CHP-DHN plant schematics (current configuration).

2.3. Demand-side flexibility enabler

The third flexibility instrument that is evaluated concerns the involvement of the final users connected to the DHN. In particular, the analysis aims to estimate the impact of the management of the TCLs of the users connected to the network. These have been modeled on the basis of the assumption that it is possible to require programmed variations of the users' setpoint at certain times of the day. The method identified to involve users is linked to the architecture of the system. In particular, as it will be described in more detail in Section 3 where the case study is introduced, the efficiency of the CHP plant in Osimo does not have at present a strong dependency on the ambient temperature without presence of intermittent renewable energy sources. For this reason, it has been considered not relevant to apply load shifting strategies to unlock the demand side flexibility.

However, looking at the available data, it was observed that the city of Osimo has an extensive photovoltaic generation plant (PV), which impacts the electric power exchange with the national grid throughout the year. Only in April 2018, the excess of electricity generation produced by PV was about 21.7% of the total electricity produced.

In view of this, given the relationship between electric and thermal energy generation in the CHP plant, the possibility to act on the users' thermal demand during the periods when there is an overproduction in PV electricity has been envisaged. More specifically, it is considered the modification of the setpoint of the users in order to reduce the thermal demand. The objective is to evaluate the impact of activating the users' flexibility on the chance of increasing the self-consumption of PV energy by avoiding the further electricity production of the CHP. This latter strategy is closely linked to the architecture of the system and it will be more clearly explained in the results section (Section 5), after both the CHP-DHN plant under study (Section 3) and the model (Section 4) are described.

3. Description of the CHP-DHN plant

In this section a description of the CHP-DHN plant considered in the study is reported. As mentioned, we refer to a real system located in Osimo, in Central Italy (43°29′ N, 13°29′ E). The following subsections report the description of the plant (Subsection 3.1) with a focus on the current operation strategies and the planned improvement interventions (Subsection 3.2).

3.1. The CHP-DHN plant

The current CHP is composed of a natural gas engine cogeneration system with an electrical nominal power of 1.2 MW_{el} and a thermal power of 1.3 MW_{th}. The plant is also equipped with natural gas boilers (2 boilers of 4.6 MW_{th} and 1 boiler of 4.2 MW_{th}, one of them used as back up) which provide additional thermal energy when the demand exceeds the engine capacity. The thermal energy produced by the CHP plant is used to produce hot water to supply a DHN (of about 444 m^3 of water) by means of a plate heat exchanger. A detailed description of the DHN under study is reported in [32], however, in this section its main features will be repeated in order to facilitate the understanding of the analysis.

The DHN connects 1265 users of which 94% are residential buildings (53% of the total thermal energy demand) and the remaining 6% are public/commercial customers (47% of the total thermal energy demand). The DHN is composed of polyurethane insulated pipes and pressurized hot water (16 bar) is used as heat transfer fluid.

The current configuration of the plant provides a direct heat exchange between the CHP and the DHN (no thermal storage system is installed).

In Fig. 2 the duration curves of the DHN total thermal demand are reported (data referred to year 2018). It is clear that the CHP is sized to cover the baseload thermal demand. Indeed, the thermal load of the DHN is greater than 1.3 MW_{th} for about 55% of the time. Furthermore, a large difference in terms of amplitude of thermal demand is recorded

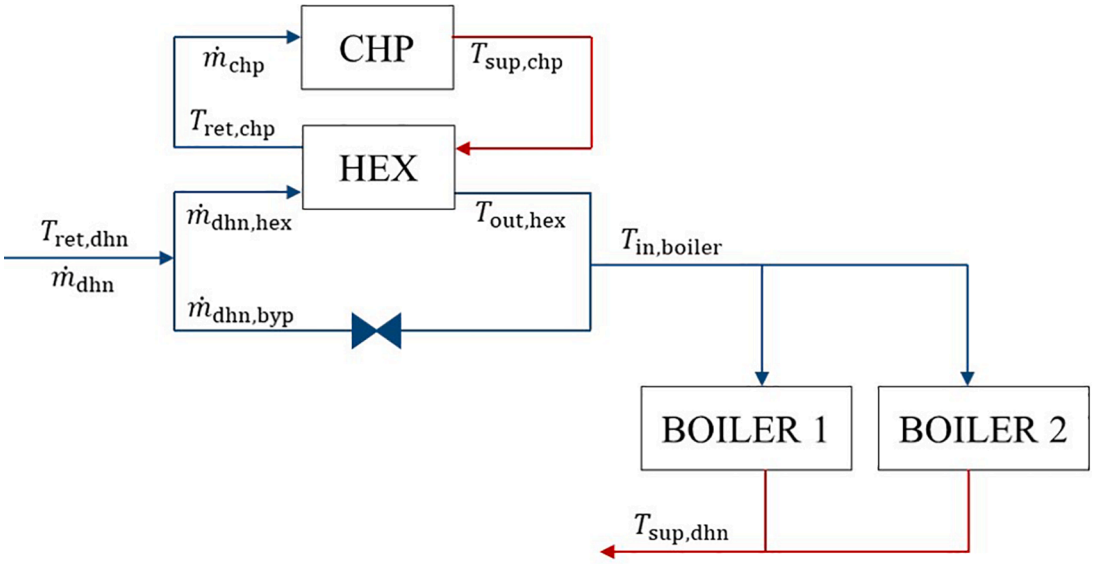

Fig. 4. CHP model schematic (current configuration).

between the winter (from November to March), mid-season (form April to mid-June and from mid-September to October) and summer months (from mid-June to mid-September). In particular a large reduction in thermal demand occurs from the winter to the summer months. In the latter in fact, the thermal power in the DHN is used only for domestic/sanitary hot water production and to dispose of thermal losses. This aspect influences the management strategy of the cogeneration plant, scarcely used now during the warm season for its reduced performance.

3.2. Current control strategies and planned interventions

As mentioned, the CHP engine is sized to cover the baseload thermal demand to maximize the hours of engine operation, especially in the winter season (Fig. 2). Currently, the heat load is supplied to the DHN at different temperatures, varied accordingly with season. The supply water temperature is adjusted to compensate the demand and the thermal losses with a rule of thumb method. In particular, in winter the supply water temperature is about 95 °C and the engine is always on together with the boilers, which provide additional demand and increase the maximum temperature achievable by the engine. During mid-season the supply water temperature ranges between 78 °C and 85 °C, the engine modulates its load on the basis of the demand (its load can be reduced down to 80% of the full capacity). In this case it has been observed that, especially at night, the CHP is found to work with a modulation lower than 60%. To avoid such lowering, a working schedule is imposed for the engine: the CHP is switched on between 7.00 am and 8.00 pm, while in the remaining hours only the boilers are used. In summer the engine is switched off and the thermal load is produced entirely by the boilers at 75 °C. As shown schematically in Fig. 3, the current set-up of the system requires that the CHP, if in operation, is the first to intervene to increase the temperature of the DHN. Subsequently, the boilers are switched on in parallel until the required supply temperature is reached.

At present, the engine start-up and shutdown working strategies are decided in order to maximize the achievable national incentives (base on primary energy saving, PES in Equation (1), that has to be higher than 10) and to prevent the engine from working below 80% of its rated power. To increase the operational hours of the CHP during mid and summer seasons and to reduce the load modulation, the addition of a TES on the engine circuit is planned. A stratified hot water tank was selected. To maximize the volume and taking into account the space constraints for its installation, a cylindrical tank of 80 m^3 (diameter of 3200 mm and height of 12000 mm) with a high level of thermal insulation (100 mm high density polyurethane, U-Value of the TES of 0.22 W m^2K^{-1}) was chosen.

4. Simulation models

In this section the simulation models to reproduce the operation of the CHP-DHN system located in Osimo are presented. The models are realized in Python with a mixed approach dictated by the availability of measured data. In particular, some parts of the plant are represented with purely data driven models, while for other parts physically based models are used. To test the reliability of the model, in this latter case, a calibration of the results with available measures is carried out (Section 5).

4.1. Model of the CHP: Current configuration (without TES)

As described in Section 3, the current configuration of the CHP plant provides a natural gas engine cogeneration system equipped with two back up natural gas boilers. Fig. 4 reports a schematic of the modelled cogeneration plant.

The total thermal demand ($\dot{Q}_{dhn}$) of the district heating network, which the generation plant has to produce, is evaluated with Equation (7): the thermal generation plant provides heat to the transfer fluid to rise its return temperature ($T_{ret,dhn}$) up to a given supply temperature setpoint ($T_{sup,dhn}$).

$$\dot{Q}_{dhn} = \dot{m}_{dhn} c_p \left(T_{sup,dhn} - T_{ret,dhn}\right) \quad (7)$$

The CHP exchanges heat through a heat exchanger that recovers heat both from the cooling system of the engine and from the waste gases (HEX in Fig. 4). If the demand is less than the maximum capacity of the CHP ($\dot{Q}_{max,chp}$ equal to 1.3 MW_{th}) then the exchangeable thermal power ($\dot{Q}_{hex,max}$)is equal to $\dot{Q}_{dhn}$, otherwise it is limited by $\dot{Q}_{max,chp}$. The remaining demand is provided by the boilers. In order to calculate the flowrate that can be elaborated by the HEX and the actual exchanged thermal power ($\dot{Q}_{hex}$), the maximum temperature allowed for the water ($\dot{m}_{dhn,hex}$)leaving the HEX is set to 80 °C ($T_{out,hex}$). Therefore:

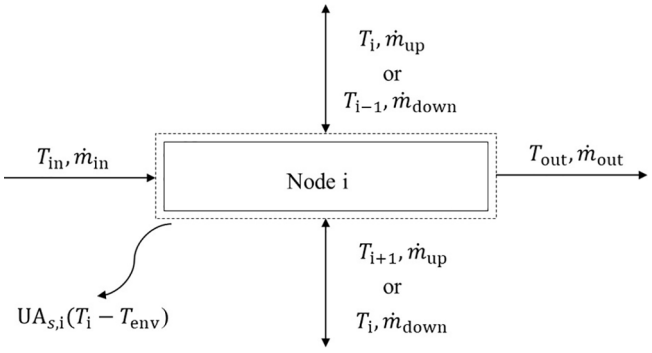

Fig. 5. Interaction with the surroundings of a single node.

$$\begin{cases} \dot{m}_{dhn,hex} = \dfrac{\dot{Q}_{hex,max}}{c_p\left(T_{out,hex} - T_{ret,dhn}\right)} \text{ and } \dot{Q}_{hex} = \dot{Q}_{hex,max} \text{ if } \left(\dfrac{\dot{Q}_{hex,max}}{c_p\left(T_{out,hex} - T_{ret,dhn}\right)}\right) < \dot{m}_{dhn} \\ \dot{m}_{dhn,hex} = \dot{m}_{dhn} \text{ and } \dot{Q}_{hex} = \dot{m}_{dhn} c_p\left(T_{out,hex} - T_{ret,dhn}\right) \text{ if } \left(\dfrac{\dot{Q}_{hex,max}}{c_p\left(T_{out,hex} - T_{ret,dhn}\right)}\right) \geq \dot{m}_{dhn} \end{cases} \tag{8}$$

The flowrate that cannot go through the heat exchanger HEX ($\dot{m}_{dhn,byp}$)is calculated as difference between the total needed flow rate ($\dot{m}_{dhn}$) and the maximum flow rate for the HEX ($\dot{m}_{dhn,hex}$).

The boiler inlet temperature is given by the (adiabatic) mixing between the two fluids ($\dot{m}_{dhn,hex}$and $\dot{m}_{dhn,byp}$). Within the CHP plant, the return temperature ($T_{ret,chp}$) for the water entering in the CHP circuit ($\dot{m}_{chp}$), is given by $T_{out,hex}$ increased of a fixed ΔT_{hex} (assumed equal to 5 °C) to ensure the effectiveness of the heat exchange:

$$T_{ret,chp} = T_{out,hex} + \Delta T_{hex} \tag{9}$$

The water flowrate $\dot{m}_{chp}$ is assessed to maintain a temperature difference between demand and supply of 20 °C (in design condition, return temperature of about 65 °C and supply of 85 °C in the CHP circuit).

As mentioned in Section 3, the existing operating control logic of the generation plant differs according to the season. Consequently, according to the available measured data referring to the year 2018, the value of $T_{sup,dhn}$ is fixed to 95 °C for the winter months (November-March) and the CHP engine is always switched on. For the mid-season months (April-mid June and mid-September-October) $T_{sup,dhn}$ is fixed to 85 °C and the engine modulates its load on the basis of the demand and the working schedule is between 7.00 am and 8.00 pm. In summer months (mid-June-mid- September) the CHP engine is turned off (only the boilers cover the demand) and the supply temperature $T_{sup,dhn}$ is set to 75 °C.

In order to represent the performance of the generation units (CHP and boilers), data driven models based on measured data are prepared. The CHP model can accurately predict gas consumption ($\dot{V}_{NG,chp}$), electrical power ($\dot{P}_{chp}$), electrical and thermal efficiency ($\eta_{el,chp}$and $\eta_{th,chp}$) having the thermal demand ($\dot{Q}_{chp}$) as input. The model provides load curves capable of evaluating the performance of the device as a function of thermal demand and external conditions. These curves are obtained with Curve Fitting Matlab toolbox [34], which assesses the coefficients of the polynomial equation describing their trend. In this sense, the electrical power produced by the CHP can be calculated with:

$$\dot{P}_{chp} = 0.9595 \cdot \dot{Q}_{chp} + 3.3531 \tag{10}$$

Knowing the thermal input power ($\dot{Q}_{chp}$) and the outside ambient temperature (T_o), the thermal efficiency of the machine ($\eta_{th,chp}$) can be evaluated:

$$\eta_{th,chp} = -0.01066 + 0.008915 \cdot \dot{Q}_{chp} + 0.001183 \cdot T_o - 4.544 \cdot 10^{-5} \cdot \left(\dot{Q}_{chp}\right)^2 - 7.05 \cdot 10^{-6} \cdot \dot{Q}_{chp} \cdot T_o - 2.803 \cdot 10^{-5} \cdot (T_o)^2 \tag{11}$$

Similarly, the electric efficiency ($\eta_{el,chp}$) is expressed in Equation (11) as function of thermal input power ($\dot{Q}_{chp}$) and outside ambient temperature (T_o):

$$\eta_{el,chp} = -6.81295 \cdot 10^{-4} + 0.00956 \cdot \dot{P}_{chp} + 6.39961 \cdot 10^{-5} \cdot T_o - 5.5346 \cdot 10^{-5} \cdot \left(\dot{P}_{chp}\right)^2 - 2.4418 \cdot 10^{-6} \cdot \dot{P}_{chp} \cdot T_o - 1.3510 \cdot 10^{-6} \cdot (T_o)^2 \tag{12}$$

It is possible to calculate the fuel (i.e. natural gas, NG) flow rate ($\dot{V}_{NG,chp}$)needed to run the CHP and produce the requested thermal power (the lower heating value, H_f, of natural gas is assumed at 33840 kJ Sm^{-3}).

$$\dot{V}_{NG,chp} = \frac{\dot{Q}_{chp}}{\eta_{th,chp} \cdot H_f} \tag{13}$$

As far as the boilers are concerned, the same approach is used, and a data driven model is derived. It represents the dependency between the thermal efficiency ($\eta_{th,boiler}$) and the thermal demand the boilers have to cover (i.e. the total thermal demand subtracted the power provided by the CHP,$\dot{Q}_{boiler}$):

$$\eta_{th,boiler} = -2.2338 \cdot 10^{-15} \cdot \left(\dot{Q}_{boiler}\right)^9 + 9.8768 \cdot 10^{-13} \cdot \left(\dot{Q}_{boiler}\right)^8 - 1.8452 \cdot 10^{-10} \cdot \left(\dot{Q}_{boiler}\right)^7 + 1.8926 \cdot 10^{-8} \cdot \left(\dot{Q}_{boiler}\right)^6 - 1.156 \cdot 10^{-6} \cdot \left(\dot{Q}_{boiler}\right)^5 + 4.2365 \cdot 10^{-5} \cdot \left(\dot{Q}_{boiler}\right)^4 - 8.7083 \cdot 10^{-4} \cdot \left(\dot{Q}_{boiler}\right)^3 + 7.5 \cdot 10^{-3} \cdot \left(\dot{Q}_{boiler}\right)^2 + 3.510 \cdot 10^{-2} \cdot \dot{Q}_{boiler} + 1.6755 \cdot 10^{-4} \tag{14}$$

Also in this case the fuel (i.e. natural gas, NG) flow rate ($\dot{V}_{NG,boiler}$)for boilers can be assessed with:

$$\dot{V}_{NG,boiler} = \frac{\dot{Q}_{boiler}}{\eta_{th,boiler} \cdot H_f} \tag{15}$$

4.2. Model of the CHP: New configuration (with TES)

As mentioned in Section 3, the TES is conceived to be connected with the CHP. As foreseen by the project, the TES is modelled as a 80 m^3 cylinder tank with a working temperature range of 65–85 °C, from which follows a design thermal energy capacity of about 6700 MJ.

A purely physical approach is used to model the thermal dynamic of

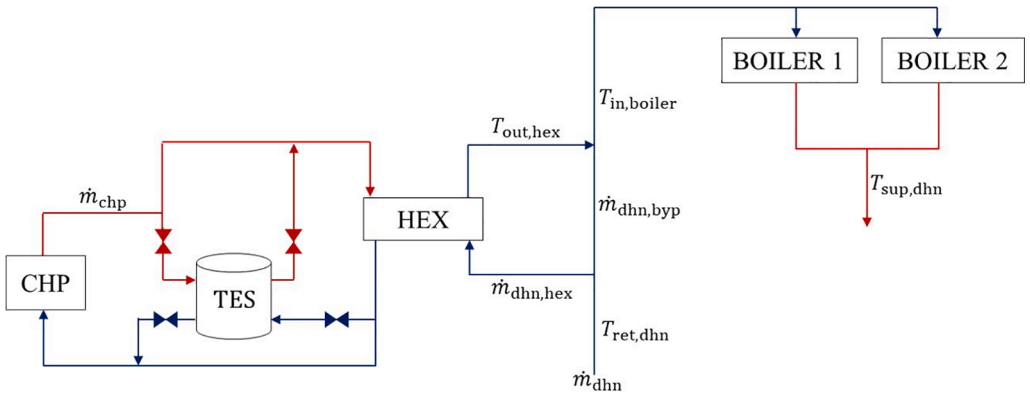

Fig. 6. Generation model schematic (with TES).

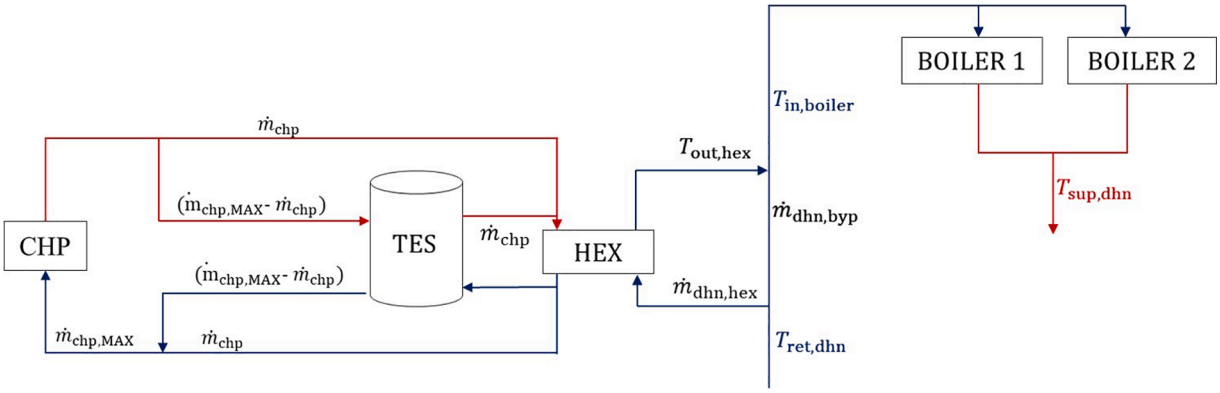

Fig. 7. CHP model with TES operating in charging mode.

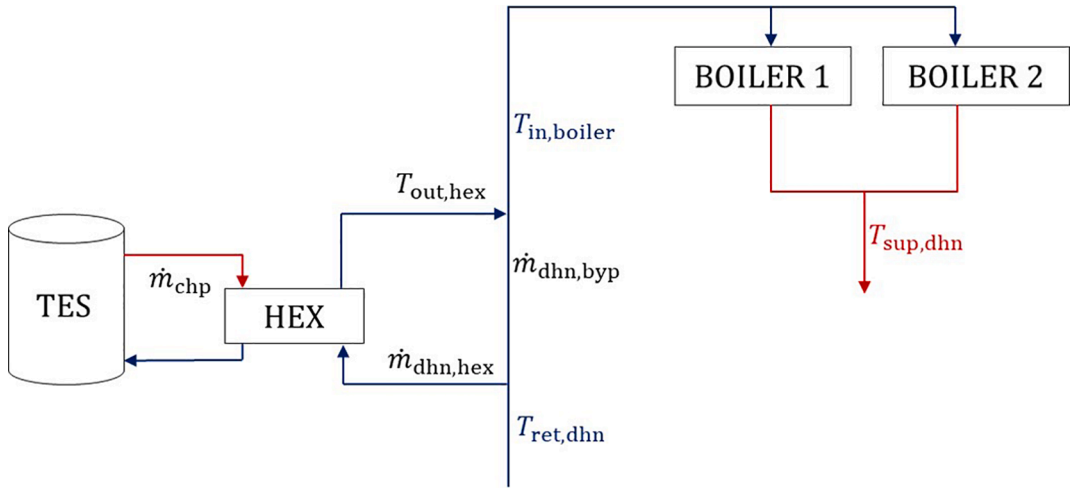

Fig. 8. CHP model with TES operating in discharging mode.

the tank since no measured data are available. In particular it is modelled as a stratified hot water tank with a multi-node 1D model approach [35]. 16 fully mixed equal volume segments are used to determine the thermal stratification. The water flow from the DHN side enters at the bottom of the tank while the hot source stream from the CHP enters at the top (flow streams enter the tank at fixed positions). The model is based on the following assumptions: (i) the fluid streams flowing up and down from each node are fully mixed before they enter each segment; (ii) the temperature is considered uniform in each node (only the vertical gradient of the temperature in the tank in represented, while the horizontal gradient is neglected); (iii) convective heat exchange between fluid segments is neglected and (iv) the thermophysical properties of the water (density and specific heat) are assumed constant.

The energy and mass exchange of a single node with the surroundings is illustrated in Fig. 5, while Eqs. (16) and (17) report the mass and energy conservation equations respectively.

$$\frac{dM}{dt} = \sum \dot{m}_{in} - \sum \dot{m}_{out} = 0 \tag{16}$$

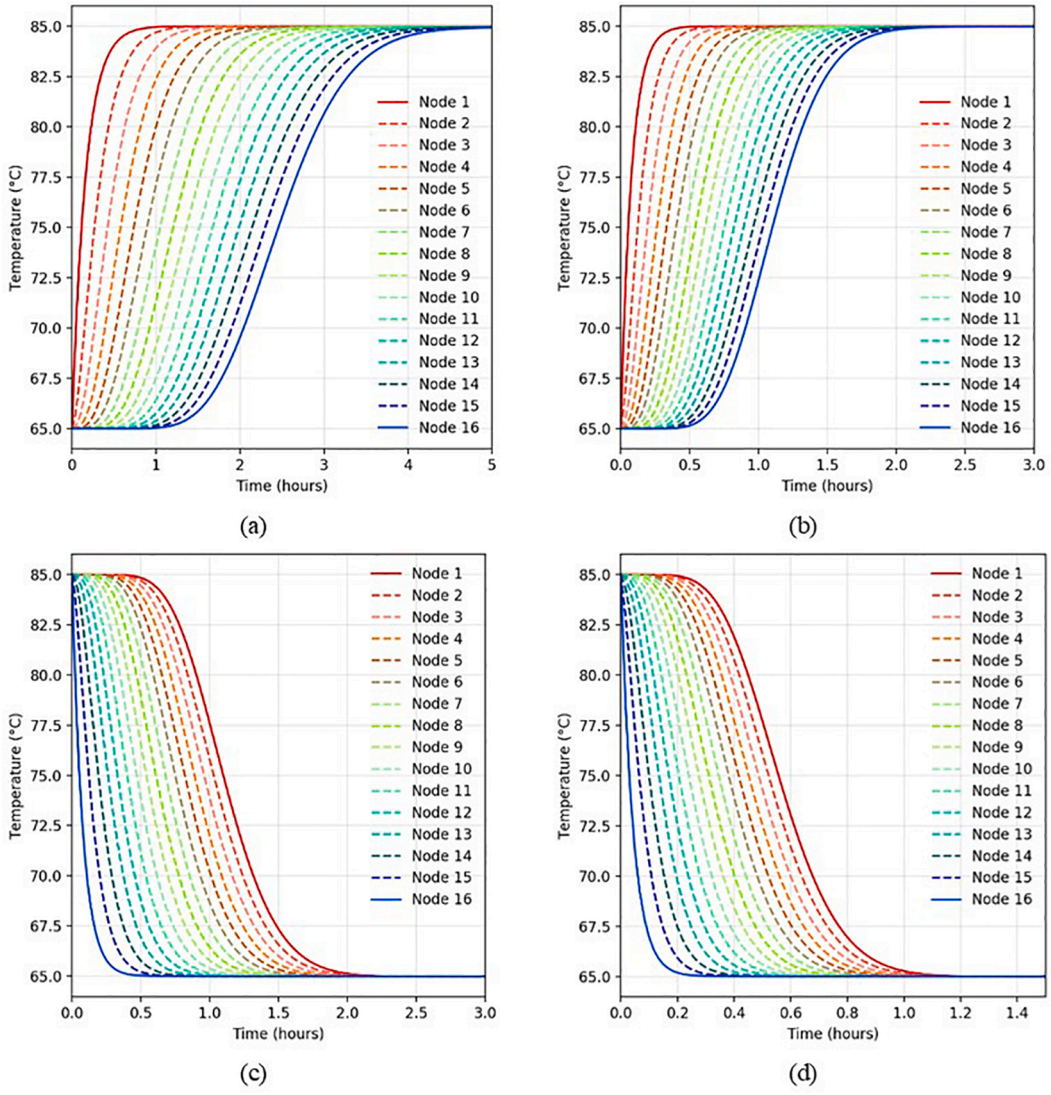

Fig. 9. Evaluation of the TES model in fixed flowrate conditions: (a) charge phase with $\dot{V}_{chp}$ of 30 m^3 hr^{-1}, (b) charge phase with $\dot{V}_{chp}$ of 60 m^3 hr^{-1}, (c) discharge phase with $\dot{V}_{dhn,hex}$ of 60 m^3 hr^{-1} and (d) discharge phase with $\dot{V}_{dhn,hex}$ of 100 m^3 hr^{-1}.

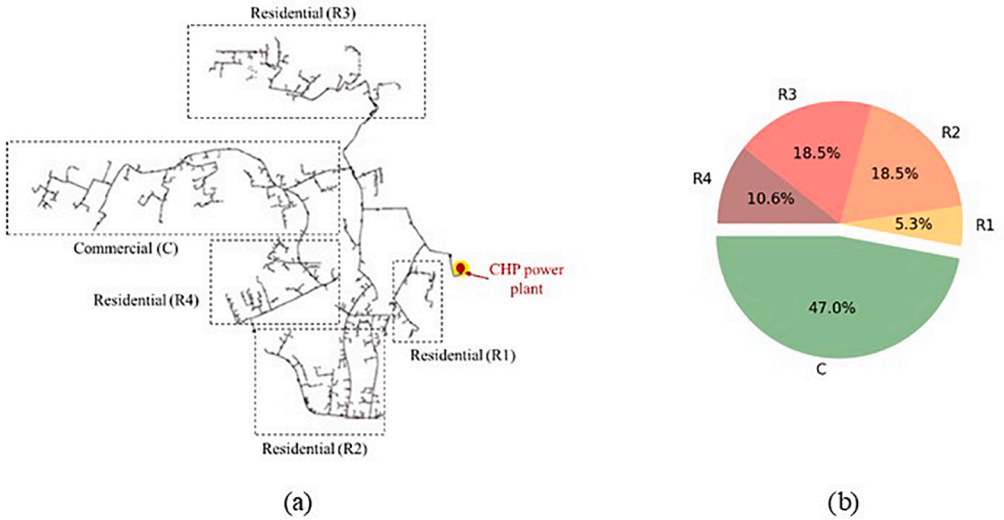

Fig. 10. Distribution of thermal demand between different clusters of users: (a) DHN layout and clusters of users identified for modelling the network and (b) percentage of impact of individual users.

Table 1
L_u-values (kW K^{-1}) for the single residential users in the different clusters.

Type of user	R1	R2	R3	R4
Residential user (a)	10.6	37.2	37.2	21
Residential user (b)	5.3	18.6	18.6	10.5
Residential user (c)	5.3	18.6	18.6	10.5
Total	21.2	74.4	74.4	42

Table 2
L_u-values (kW K^{-1}) for the single commercial users.

Type of user	C
Commercial user (a)	94
Commercial user (b)	94
Total	188

Table 3
Values of $\dot{Q}_{bl}$ (kW_{th}) assigned in the various periods of the year.

Period of the year	$\dot{Q}_{bl}$ (kW_{th})
From 1 January to 31 March	1300 (24 h a day)
From 1 April to 18 April	800 (24 h a day)
From 18 April to 31 May	• 1400 (from 5.00 am to 8.00 am and from 6.00 pm to 8.00 pm) • 750 (from 8.00 am to 6.00 pm) • 450 (remaining hours)
From 1 June to 15 June	• 1000 (from 5.00 am to 8.00 am and from 6.00 pm to 8.00 pm) • 500 (from 8.00 am to 6.00 pm) • 250 (remaining hours)
From 15 June to 15 September	• 650 (from 5.00 am to 8.00 am and from 6.00 pm to 8.00 pm) • 450 (from 8.00 am to 6.00 pm) • 200 (remaining hours)
From 15 to 30 September	• 1000 (from 5.00 am to 8.00 am and from 6.00 pm to 8.00 pm) • 500 (from 8.00 am to 6.00 pm) • 250 (remaining hours)
From 1 October to 18 November	• 1400 (from 5.00 am to 8.00 am and from 6.00 pm to 8.00 pm) • 750 (from 8.00 am to 6.00 pm) • 450 (remaining hours)
From 18 November to 31 December	1300 (24 h a day)

$$\frac{dE}{dt} = \sum h_{in}\dot{m}_{in} - \sum h_{out}\dot{m}_{out} + \sum \dot{Q}_i = 0 \quad (17)$$

Considering M as the mass of water contained in the single node *i*, Equation (16) can be rewritten:

$$Mc_p\frac{dT_i}{dt} = \dot{m}_{in}c_pT_{in} - \dot{m}_{out}c_pT_{out} + \dot{m}_{f,in}c_pT_{f,in} - \dot{m}_{f,out}c_pT_{f,out} + UA_{s,i}(T_{env} - T_i) \quad (18)$$

Where U is the thermal transmittance of the TES, $A_{s,i}$ the dispersing area of the single node i and T_{env} the temperature of the environment in which the tank is located. Referring to Equation (18), if the water is flowing downwards, the following assumptions apply:

$$\dot{m}_{f,in} = \dot{m}_{down}, \dot{m}_{f,out} = \dot{m}_{down}$$

$$T_{f,in} = T_{i-1}, T_{f,out} = T_i \quad (20)$$

While, if the water is flowing upwards:

$$\dot{m}_{f,in} = \dot{m}_{up}, \dot{m}_{f,out} = \dot{m}_{up}$$

$$T_{f,in} = T_{i+1}, T_{f,out} = T_i \quad (22)$$

The integration of the TES in the system is represented in the schematic in Fig. 6.

The CHP can charge the TES when the thermal demand is lower than the CHP maximum thermal capacity. After it has been fully charged, the TES can be discharged following a specific control logic, while the CHP is maintained off. The following Figs. 7 and 8 show the operational phases of the TES and the corresponding hydraulic configurations. The charging and the discharging phases are as follows:

- Charging phase: the TES is considered charged when the lower node reaches the temperature of 67 °C. The latter temperature setpoint is

Table 4
Monthly comparison between measured data (2018) and simulations: total heating demand.

Month	Data (MWh_{th})	Simulation (MWh_{th})	Variation
January	3099	3180	3%
February	3438	3471	1%
March	3115	3035	−3%
April	1323	1365	3%
May	864	900	4%
June	691	646	−7%
July	525	599	12%
August	565	560	−1%
September	665	696	4%
October	884	952	7%
November	1951	1984	2%
December	3244	3382	4%

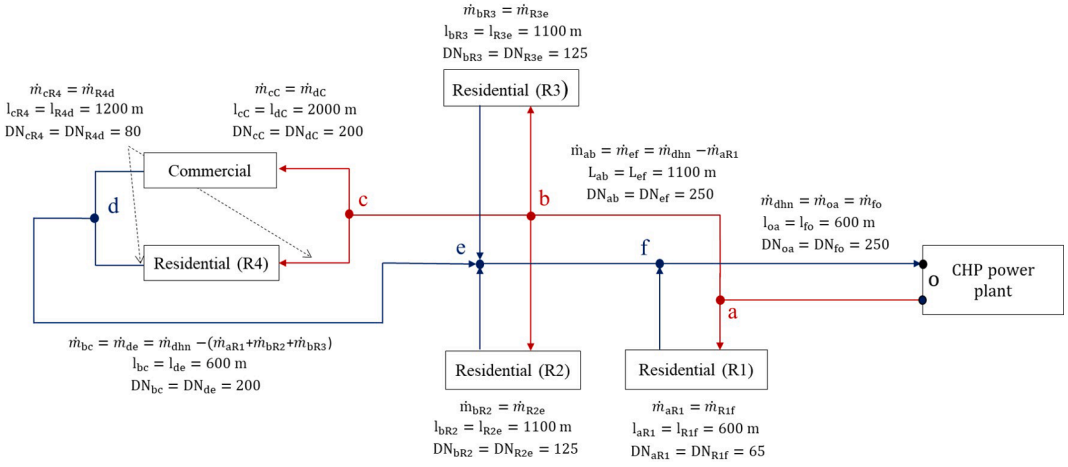

Fig. 11. DHN model scheme.

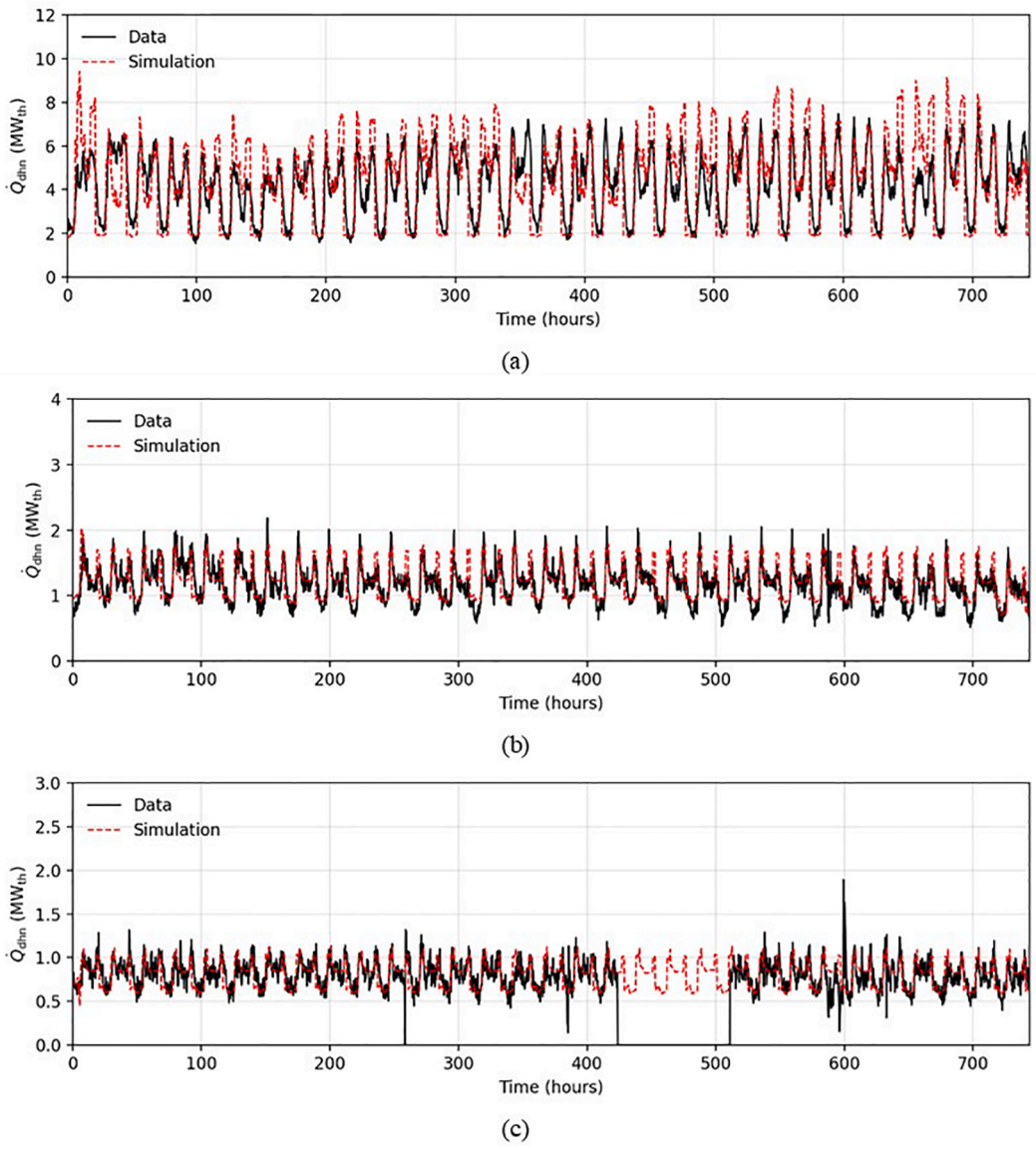

Fig. 12. Monthly comparison between measured data (2018) and simulations: total heating demand: (a) January, (b) May and (c) July.

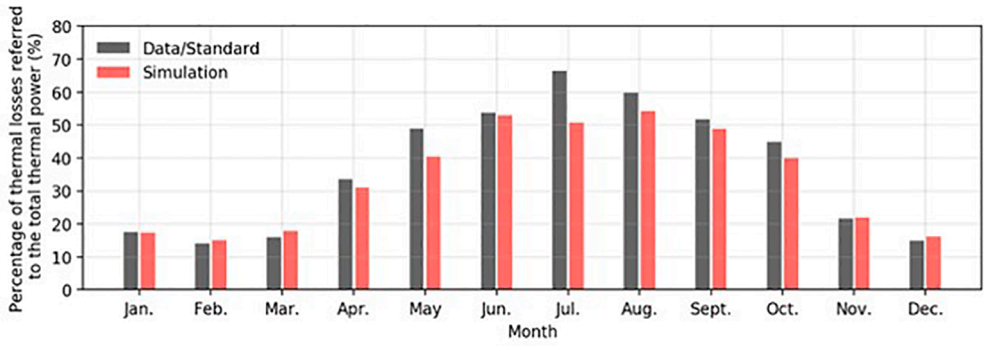

Fig. 13. Monthly comparison between measured data (2018) combined with calculation according to [38] and simulations: percentage of thermal losses to total thermal demand.

selected to guarantee a minimum temperature difference with the carrier delivering heat from the CHP (Fig. 7).

- Discharging phase: the TES is considered fully discharged when the upper node reaches the temperature of 67 °C (Fig. 8).

It is important to notice that the modelled operation logic of the TES is the one hypothesized in the design phase. However, the tank has not yet been installed.

Fig. 9 shows the temperature trends in the different thermal nodes during charging and discharging phase. To test the operation of the TES

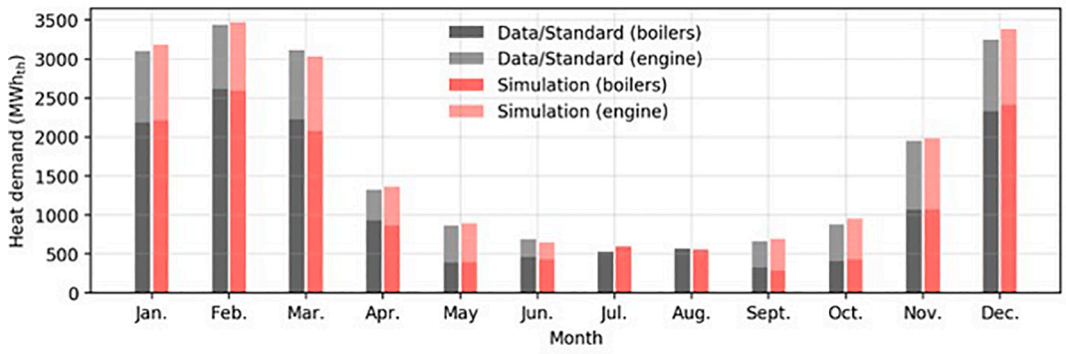

Fig. 14. Monthly comparison between measured data (2018) and simulations: heating demand covered by CHP engine and boilers.

Table 5
Monthly comparison between measured data (2018) and simulations: electricity (CHP engine) and total NG consumption.

Month	Electricity produced by CHP			Total fuel consumption (NG)		
	Data (MWh_{el})	Simulation (MWh_{el})	Variation	Data (Sm^3)	Simulation (Sm^3)	Variation
January	882	931	5%	485,576	489,869	1%
February	798	841	5%	511,272	507,425	−1%
March	876	917	4%	479,196	472,583	−1%
April	386	484	20%	208,824	231,367	10%
May	464	484	4%	166,894	179,517	7%
June	232	208	−12%	112,130	116,164	3%
July	0	0	–	64,920	80,124	19%
August	0	0	–	62,267	81,951	24%
September	341	397	14%	128,139	146,837	13%
October	464	502	8%	169,092	186,424	9%
November	842	874	4%	342,623	356,747	4%
December	880	930	5%	498,430	495,691	−1%

model, two different values of flowrates (fixed values) coming from the CHP plant are considered based on the operational ranges allowed by the water pumps foreseen in the circuit. They are the minimum and maximum volumetric flow rates during the charging phase ($\dot{V}_{chp}$): 30 m^3 $h^{-1}$and 60 m^3 h^{-1}, while during the discharging phase they are 60 m^3 h^{-1} and 100 m^3 h^{-1} ($\dot{V}_{dhn,hex}$). Depending on the flowrates, the TES is charged in a range between 39 and 90 min and discharged between 56 and 107 min.

4.3. Model of the DHN

To model the dynamic of the district heating network a mixed approach is adopted on the basis of the available data. The thermal model of the pipes is realized with a purely physically approach while the users demand is modelled with simple linear equations that allow to take into account the dependence of the demand on the external and on the internal temperature setpoint of the users. For the latter case, the equations are calibrated on the basis of the available measurements. For clarity, the modeling procedure will be described in detail below.

Analyzing the available data and the information about the users (Section 3), it is possible to identify 5 main clusters of final users in the different branches of the network: 4 of these clusters contains residential (R) users, while one mostly commercial user (C). In Fig. 10a a map representing the DHN layout is shown. Considering that, commercial users account for 47% of the total thermal demand, while the residential users constitute the remaining 53%, the following weights are assigned to the various clusters of residential users (referring to the total domestic thermal demand): 10% for R1, 35% for R2, 35% for R3 and 20% for R4. In particular, the cluster R3 refers to residential users located in the historic center of the city. Fig. 10b represents the total thermal demand distribution among the different clusters, as assumed for modelling the grid based on available data.

The thermal demand of each cluster ($\dot{Q}_u$) is modelled through Equation (23). It is obtained as the sum of a variable contribution ($\dot{Q}_{vl}$) that stands for the space heating demand, and a baseload ($\dot{Q}_{bl}$) that represents the demand for domestic hot water. Since the city of Osimo is located in the Italian climatic zone D (2073 GG), $\dot{Q}_{vl}$ is present only from November 1st to April 15th (duration of the heating season). $\dot{Q}_{vl}$ is expressed as a function of the outside environment temperature (T_o) and of the indoor temperature setpoint T_{sp} (a value of 20 °C is assumed). L_u represents the thermal load coefficient of the user expressed in (W K^{-1}), while *Ctrl* is the control of the system (1 on, 0 off).

$$\dot{Q}_u = \dot{Q}_{vl} + \dot{Q}_{bl} = \left[L_u \cdot Ctrl \cdot (T_{sp} - T_o)\right] + \dot{Q}_{bl} \quad (23)$$

In order to represent a diversified thermal demand, different occupancy profiles are considered. They are chosen accordingly to the information available for the final users and they have been applied uniformly during the whole year:

- Residential user (a), *Ctrl* of 1 from 5.00 am to 9.00 pm.
- Residential user (b), *Ctrl* of 1 from 5.00 am to 10.00 am, from 12 pm to 2.00 pm and from 5.00 pm to 9.00 pm.
- Residential user (c), *Ctrl* of 1 from 5.00 am to 10.00 am and from 5.00 pm to 9.00 pm.
- Commercial user (a), to consider small businesses, *Ctrl* of 1 from 7.00 am to 1.00 pm and from 4.00 pm to 9.00 pm.
- Commercial user (b), to consider small businesses, *Ctrl* of 1 from 7.00 am to 9.00 pm.

Each cluster of residential users is assumed composed of 50% users of type (a), 25% of type (b) and finally 25% of type (c). Regarding the commercial user cluster: 50% of the users are of type (a) while the remaining 50% is of type (b). Using the available measured data, the total value of 400 W K^{-1} is obtained for the thermal load coefficient.

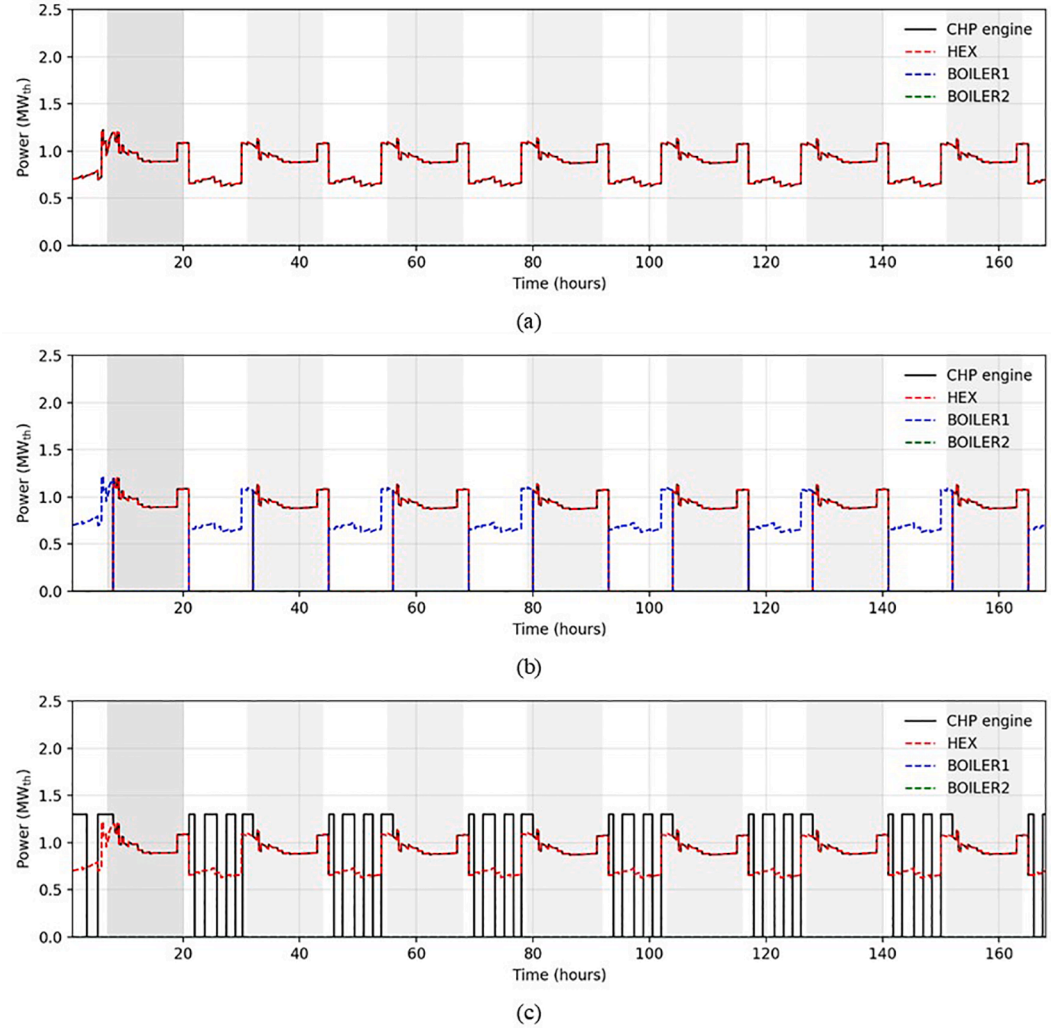

Fig. 15. Weekly thermal demand covered by CHP, exchanged by the CHP heat exchanger (HEX in Fig. 6) and covered by boilers: (a) CHP always running, (b) CHP on from 7.00 am to 8.00 pm and without TES and (c) CHP on from 7.00 am to 8.00 pm and TES working in the other hours.

Therefore, the values of L_u for each cluster are calculated by multiplying the total value of the thermal load coefficient for the weight of the corresponding cluster (Fig. 10b). Tables 1 and 2 report the L_u values for the residential users in the clusters and commercial users, respectively.

As far as $\dot{Q}_{bl}$ is concerned, it is only applied to residential users and its numerical value is determined from the analysis of the base load in the measured data. In detail the values assumed are reported in Table 3.

Fig. 11 shows the scheme of the DHN as modelled. To distribute the flowrate among the clusters, the percentages reported in Fig. 10b are used. The pipe diameters are evaluated to maintain the fluid velocity between 1 and 1.5 m s^{-1} based on commercial pipe diameters [36]. As far as the pipe length of the various branches is concerned, it is chosen to obtain the same overall fluid volume content (444 m^3) of the real system. A total equivalent transmittance (0.68 W m K^{-1}) is used to model the heat exchanged between the pipes and the ground. It is assessed considering the detailed calculation of thermal losses in the real DHN.

The ground temperature is evaluated through Equation (24):

$$T_{ground} = T_o + \left(T_o - T_{o,average}\right) \cdot p \tag{24}$$

where $T_{o,average}$ is the average temperature of the external environment over the period considered and p a damping factor (equal to 0.5).

As mentioned, to model the network pipes, a purely physically based model in used. In particular, a "plug-flow" model is realized [37]. This modeling technique provides that the pipe is divided into fluid segments of variable size. To represent the time of piping crossing, the fluid that enters in a timestep physically moves the position of the various segments within the pipe. The average outlet temperature is computed as the mass weighted average of leaving elements and the segments that remain inside (each at a different temperature) contribute individually to the thermal losses towards the ground ($\dot{Q}_{loss}$).

In conclusion, the definition of the DHN model allows to assess the total thermal demand ($\dot{Q}_{dhn}$) from the DHN defined in Eq. (7) distinguishing the two terms that compose it: the total thermal demand of the N users ($\dot{Q}_{u,tot}$) and the thermal losses towards the ground ($\dot{Q}_{loss}$):

$$\dot{Q}_{dhn} = \dot{Q}_{u,tot} + \dot{Q}_{loss} = \sum_{u}^{N} \dot{Q}_u + \dot{Q}_{loss} \tag{25}$$

5. Model validation: Comparison with measured data

In order to evaluate its reliability, the CHP-DHN model described in Section 4 is tested under the same operating conditions in which the measured data are available. Table 4 shows the monthly overall heat demand obtained with the model in comparison with the available data (reference scenario). Fig. 12 instead reports the hourly trend of the estimated thermal demand in different seasons (e.g., January for winter season, May for mid-season and July for summer season). Looking at Table 4, it can be noted that the variation of the model with respect to the measured data remains below 10%, except for the month of July

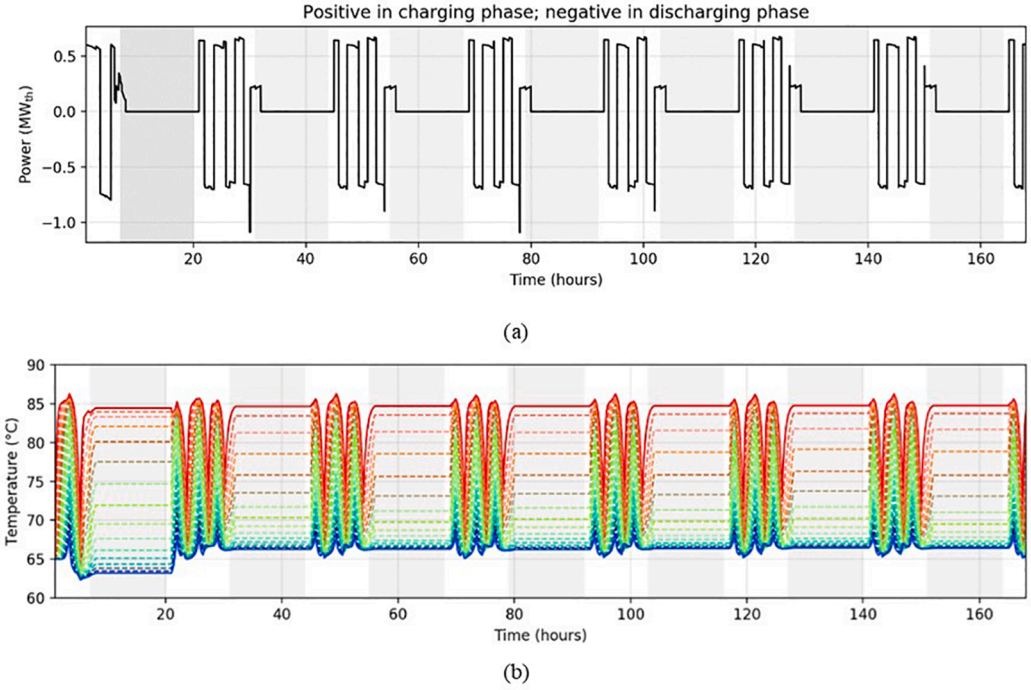

Fig. 16. (a) Thermal power exchanged by the TES and (b) Temperature of the thermal nodes of the TES.

Table 6
Performance comparison for the three considered configurations (second week of September).

Quantity	No TES CHP 24 h/ 24 h	No TES CHP on from 7.00 am to 8.00 pm	TES from 8.00 pm to 7.00 am CHP on from 7.00 am to 8.00 pm
Total demand (MWh_{th})	144.1	144.1	144.1
Thermal power CHP (MWh_{th})	144.1	86.4	145.9
Thermal power HEX (MWh_{th})	144.1	86.4	144.1
Thermal power BOILER (MWh_{th})	0	57.7	0
Electricity CHP (MWh_e)	138.8	83.4	140.6
Fuel total (m^3)	40,317	30,942	37,874
Fuel CHP (m^3)	40,317	23,033	37,874
Fuel Boiler (m^3)	–	7909	–
$\eta_{el,chp}$	0.366	0.385	0.395
$\eta_{th,chp}$	0.380	0.399	0.410
$\eta_{th,b1}$	–	0.776	–
$\eta_{th,b2}$			–
PES (%)	12.9	17.1	19.3

since the measured data are not complete and records for a few days are missing (Fig. 12c).

Regarding the network heat losses to the ground, no measure data are available. However, to test the model, the monthly simulation results are compared to the values obtained with the calculation discussed in [32], which is based on the application of the standard UNI EN ISO 12241:2009 [38]. Fig. 13 represents the monthly comparison between measured data combined with calculation and simulations in terms of percentage of thermal losses to total thermal demand. Except for the month of July, for which the estimate of losses from the norm includes the whole month while the measured data have some deficiencies (Fig. 12c), the error remains below ± 15%.

Fig. 14 illustrates in detail the heat generation side, i.e. the share of the demand satisfied by the CHP engine and by the boilers. Even in this case the variations compared to real data are lower than 10%. Bigger variations are found in the months of April and September (about 23%). However, in the latter cases it can be noted an unexpected switching off of the CHP that is not reproduced by the model.

Table 5 reports the comparison of the electricity produced by the CHP engine and the total fuel consumption. About the variations between real and simulated data, the same considerations commented in the point above about Fig. 14 applies.

The agreement between the simulated and real data is considered enough for the purposes of this analysis, which wishes to show the qualitative impact and significance of the flexibility instruments identified. The model guarantees a good trade-off between computational efforts and accuracy. This aspect is confirmed also by the hourly trend of the estimated thermal demand, as shown for some representative months in Fig. 12.

6. Results

In this section the flexibility instruments identified in Section 2 are tested by means of the simulation models presented in Section 4. As mentioned, the flexibility activations are aimed at producing improvements in the energy/environmental performance of the CHP-DHN plant described in Section 3. The flexibility instruments are: (i) the TES added to the CHP-engine water circuit (ii) the optimal management of the supply water temperatures to the DHN and (iii) the management of the TCLs of the final users. The following subsections report the results obtained for each flexibility enabler.

6.1. Thermal energy storage on the generation-side

As described in Subsection 2.2, the water TES will be included in the CHP plant in order to extend its working time. At present in winter the CHP covers the baseload demand and works at full load all the time. It is off in summer, while in mid-season the CHP works between 7.00 am and 8.00 pm, so not to reach too low partial load conditions (Subsection 3.2). The strategy tested in this section precisely concerns the evaluation of the contribution of the TES to increase the flexibility of the system in the

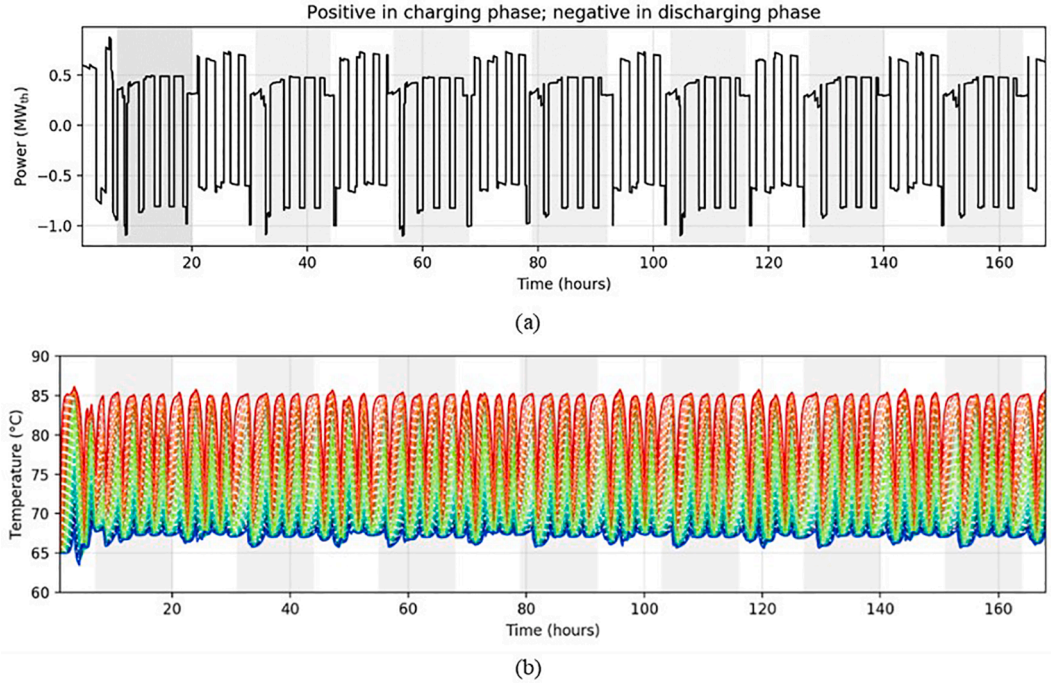

Fig. 17. (a) Thermal heating power through the TES and (b) Temperature of the thermal nodes of the TES. No schedule for CHP.

Table 7
Weekly performance calculation (first week of August) no TES.

Quantity	No CHP	No TES No Schedule CHP	No TES Schedule CHP (from 7.00 am to 8.00 pm)
Total demand (MWh_{th})	132.4	132.4	132.4
Thermal power CHP (MWh_{th})	0	132.4	79.9
Thermal power HEX (MWh_{th})	0	132.4	79.9
Thermal power BOILER (MWh_{th})	132.4	0	52.5
Electricity CHP (MWh_{el})	0	127.6	77.2
Fuel total (m^3)	17,840	38,811	29,652
Fuel CHP (m^3)	0	38,811	22,173
Fuel Boiler (m^3)	17,840	0	7479
$\eta_{el,chp}$	–	0.35	0.37
$\eta_{th,chp}$	–	0.36	0.38
$\eta_{th,b1}$	0.79	–	0.75
$\eta_{th,b2}$			.
PES (%)	–	8.6%	13.5%

Table 8
Weekly performance calculation (first week of August) with TES.

Quantity	TES from 8.00 pm to 7.00 am and Schedule CHP (from 7.00 am to 8.00 pm)	CHP with TES
Total demand (MWh_{th})	132.4	132.4
Thermal power CHP (MWh_{th})	134.1	136.5
Thermal power HEX (MWh_{th})	132.4	132.4
Thermal power BOILER (MWh_{th})	0	0
Electricity CHP (MWh_{el})	129.4	131.5
Fuel total (m^3)	35,778	34,459
Fuel CHP (m^3)	35,778	34,459
Fuel Boiler (m^3)	0	0
$\eta_{el,chp}$	0.38	0.40
$\eta_{th,chp}$	0.40	0.42
$\eta_{th,b1}$	–	–
$\eta_{th,b2}$		
PES (%)	16.5%	20.6%

warmer seasons (i.e., mid-season and summer season). Indeed, the implementation of the TES makes possible to anticipate the switching on of the CHP and to run it even when the network load is lower than the minimum required by the CHP engine. In this way, the CHP engine can work at full load, storing part of the thermal energy produced in the TES (system schematic in Fig. 6).

Starting from the analysis in mid-season, a representative week in considered (second week of September, data from 2018). Three scenarios of system operation are tested and compared in terms of performance achieved:

- CHP running 24 h/24 h: the CHP load drops also to 60% during night when the demand is lower (Fig. 15a).
- CHP switched on according to the program currently implemented (from 7.00 am to 8.00 pm), while the boilers work during night-time (Fig. 15b).
- CHP switched on in the period from 7.00 am to 8.00 pm without using the TES and CHP switched on in the remaining hours (from 8.00 pm to 7.00 am) connected with the TES (always works at full load charging the storage). In this case the thermal demand is satisfied by the CHP or by the TES (Fig. 15c) and the tank is continuously charged and discharged during night-time, as shown in Fig. 16.

Table 6 shows the energy performance of the CHP plant for the three considered configurations. To calculate the PES according to Equation (1), a reference thermal and electrical efficiency equal to 92% ($\eta_{th,rif}$) and 49.8% ($\eta_{el,rif}$) respectively were used [39], while the values of the CHP

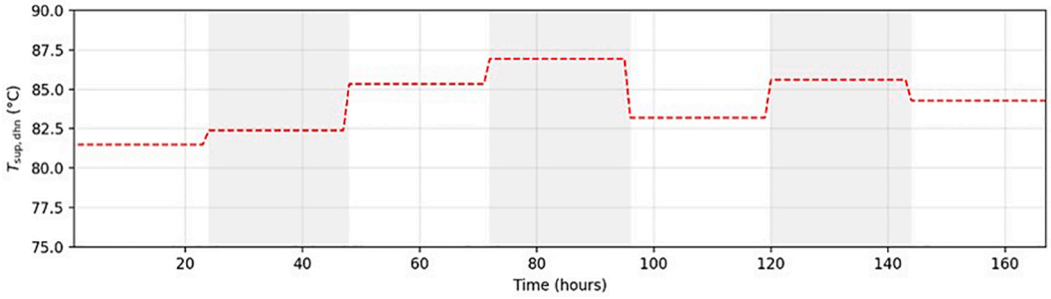

Fig. 18. Optimal daily values of the supply water temperature to the DHN in a representative winter week.

Table 9
Fuel consumption comparison between the reference scenario and the optimized scenario.

Operating scenario	V_{NG} (m^3)	$V_{NG,chp}$ (m^3)	$V_{NG,boiler1}$ (m^3)	$V_{NG,boiler2}$ (m^3)
reference	114,100	54,195	49,784	10,121
optimized	113,115	54,195	49,326	9594

efficiencies were calculated starting from the results of the simulations ($\eta_{th,chp}$and $\eta_{el,chp}$ in Table 6).

Looking at the results obtained in Table 6, it can be seen that the current configuration (No TES CHP on from 7.00 am to 8.00 pm in Table 6) allows to increase the PES by 32.6% (from 12.9% to 17.1%) compared to the configuration in which the CHP is always on (No TES CHP 24 h/24 h in Table 6). This is due to the fact that the CHP scheduling allows to avoid reduced loads, frequently at night, with a consequent increase in efficiency: both electrical and thermal efficiencies increase by 5% (Table 6). Although the current regulation in itself allows to limit the hours of operation at low modulation of the CHP with a greater exploitation of the fuel, this is not the most flexible solution, as forced CHP shutdown is required even during the hours when it could work.

The adoption of the TES increases the flexibility of the energy generation. In fact, the TES allows both to manage the operation of the CHP at maximum load, as can be seen in Figs. 15 and 16, and to further increase the performance of the congenator. Although, in the case with TES, the thermal power produced by the CHP slightly increases, due to the TES thermal losses: 145.9 MWh_{th} in case of TES (TES from 8.00 pm to 7.00 am CHP on from 7.00 am to 8.00 pm , Table 6) in comparison with of 144.1 MWh_{th} (No TES CHP 24 h/24 h), the overall performance of the plant improves. The thermal and the electrical efficiencies of the CHP increases by 8% (Table 6) while the PES (Equation (1)) reaches the value of 19.3 (49.6% increase compared to the case without TES and CHP working 24 h/24 h and 12.9% increase compared to the case without TES and CHP working from 7.00 am to 8.00 pm).

The same analysis was also performed for a summer week (first week of August). In that case the CHP at present is always off. In addition to the scenarios considered above, a fourth case was included when the CHP is always on and can work 24 h per day at full load to charge the TES (see Fig. 17).

In Tables 7 and 8 the energy performance of the CHP plant without TES and with TES, respectively, is reported. It is evident that the presence of the TES increases the primary energy saving (PES) of the cogeneration unit and allows to keep it on also in periods when a high reduction of its thermal production would have been requested.

Considering the summer week, the improvement in performance observed in the evaluations made for the mid-season is even more evident as the involvement of the TES increases. As already observed, also in this case running the CHP with a daily scheduling (from 7.00 am to 8.00 pm) would increase the PES (Equation (1)) of the CHP engine. The simulations estimate a 57% increase compared to the case in which the CHP was operated 24 h a day (from 8.6% to 13.5%, Table 7). It is also possible to observe the improvement obtained considering a functioning of the TES only during the night hours. The PES (Equation (1)) reaches the value of 16.5% (Table 8) with also an important increase in thermal and electrical efficiencies which reach the values of 0.40 and 0.38 respectively. Considering the configuration in which the TES is involved 24 h a day (CHP with TES, in Table 8), a further performance improvement can be observed. The calculated PES becomes 20.6%, while the thermal and electrical efficiencies reach the values of 0.42 and 0.40 respectively. This is due to the fact that, in the summer months the degree of modulation at which the CHP engine works during the day (from 7.00 am to 8.00 pm) is always close to the minimum threshold (60%). Therefore, the introduction of TES would allow the CHP to operate even in the summer months, confirming itself as an important flexibility tool for the system.

6.2. DHN optimal supply temperature

As mentioned in Section 3, in the current configuration of the CHP-DHN pant the supply temperature of the water is adjusted in the different seasons to compensate the demand and the thermal losses with a rule of thumb method (i.e. in winter, November-March, the supply water temperature is 95 °C; during mid-season, April- mid June and mid-September-October, the supply water temperature ranges between 78 °C and 85 °C and in summer the supply water temperature is 75 °C ,Subsection 3.2). To investigate the impact of adopting optimized daily temperature values, an optimization problem (Equation (2)) is formulated. Referring it to the plant under study, the following values can be considered: $\dot{m}_{dhn,max}$ in Equation (4) equal to 67 kg s^{-1}, $T_{sup,dhn,max}$ in Equation (5) equal to 95 °C and $T_{ret,dhn,min}$ in Equation (6) equal to 55 °C.

The obtained results are compared with a reference case where the supply water temperatures are the same as actually implemented in the plant. In Fig. 18 the optimal daily supply water temperatures in a representative winter week in Osimo are reported (first week of January 2018).

In the same week the real plant is run with a supply water temperature of 95 °C. In Table 9 the variation of the NG fuel is shown: by reducing the supply water temperature is possible to reduce the fuel consumption of about 1% in the considered week. Furthermore, given that the CHP plant covers the baseload thermal demand, it is possible to notice that the fuel consumption reduction is related to a reduction of the use of the gas boilers (Table 9).

In Fig. 19 a detailed comparison of the system dynamic in the reference and optimized scenarios is reported. It is possible to notice that the users' demand is always satisfied (Fig. 19a), while the thermal losses are reduced (Fig. 19b). The supply water temperature is reduced compared to the reference case (current operating scenario), while the return temperature does not vary significantly (Fig. 19c). The temperature reduction causes an increase of the water flowrate in order to guarantee the same thermal performance (Fig. 19d).

The results show how there is an operating margin to

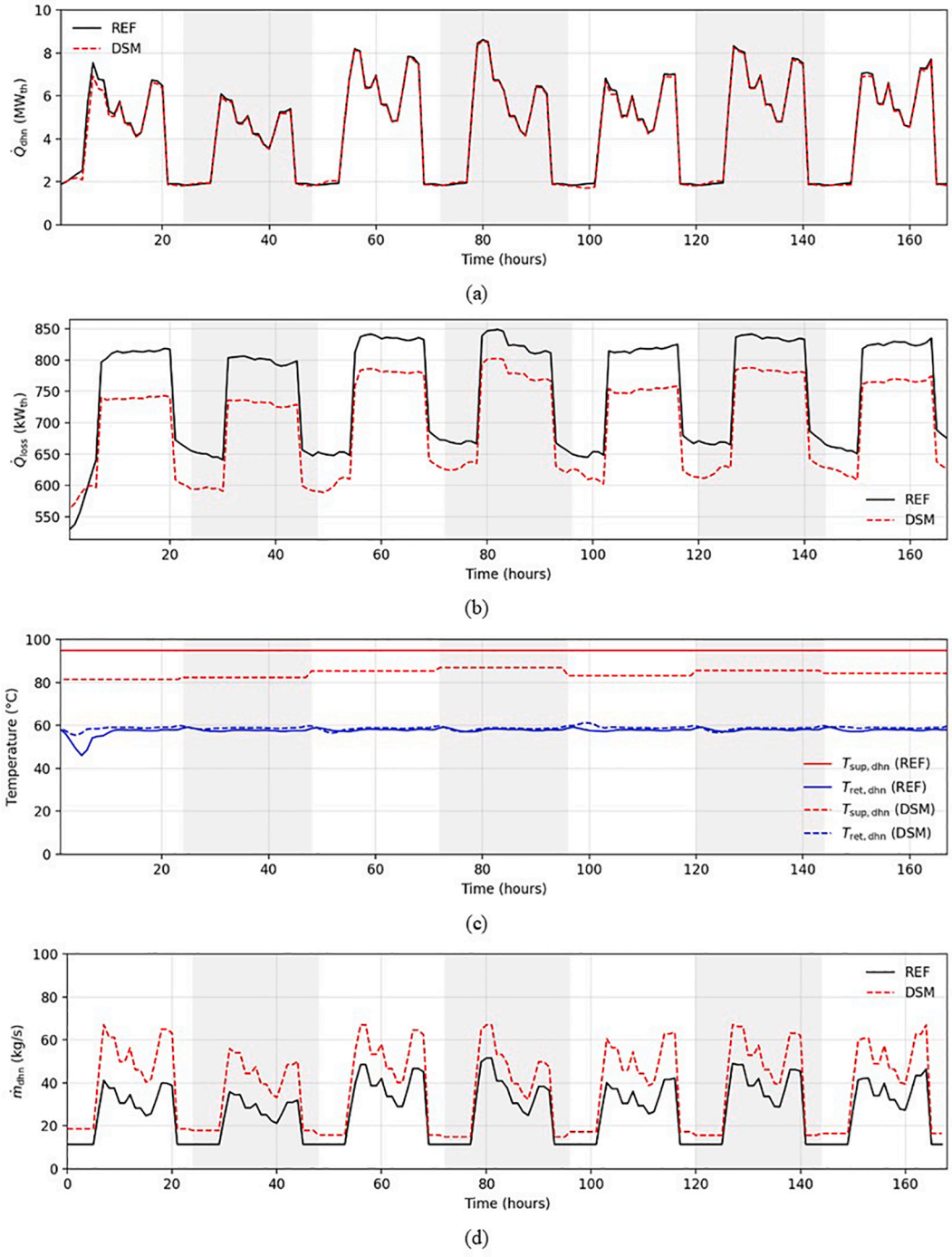

Fig. 19. Comparison between the optimized and reference scenario of: (a) DHN thermal demand, (b) thermal losses, (c) DHN supply and return temperature and (d) DHN water flowrate.

programmatically reduce the thermal demand of the system by acting with an optimized control of the water supply temperatures in the distribution system. This intervention, in addition to promoting the reduction of thermal losses in relation to the constraints to be satisfied (Table 9), can be seen as an important instrument of system flexibility. It is interesting to observe that in the summer the supply water temperature is always the lower possible for the DHN technical constraints. Even with a limited reduction of the supply temperature (from 75 °C to 70 °C), a natural gas reduction of about 2% can be achieved.

6.3. Activation of the TCLs of the final users

The purpose of this last flexibility activation is to show the influence of the management of the TCLs on the CHP plant (flexibility instrument on the demand-side). Objective of the analysis is to assess if a reduction of the space heating thermal demand during those moments can be effective to reduce the CHP thermal and electric energy production. Given that in winter the CHP is always on to cover the baseload demand (then the incidence of the space heating demand is limited), only the mid-season months, when the CHP works also at part load conditions, can be interesting for the purposes of this analysis.

Based on data measured for the year 2018, a re-injection event in

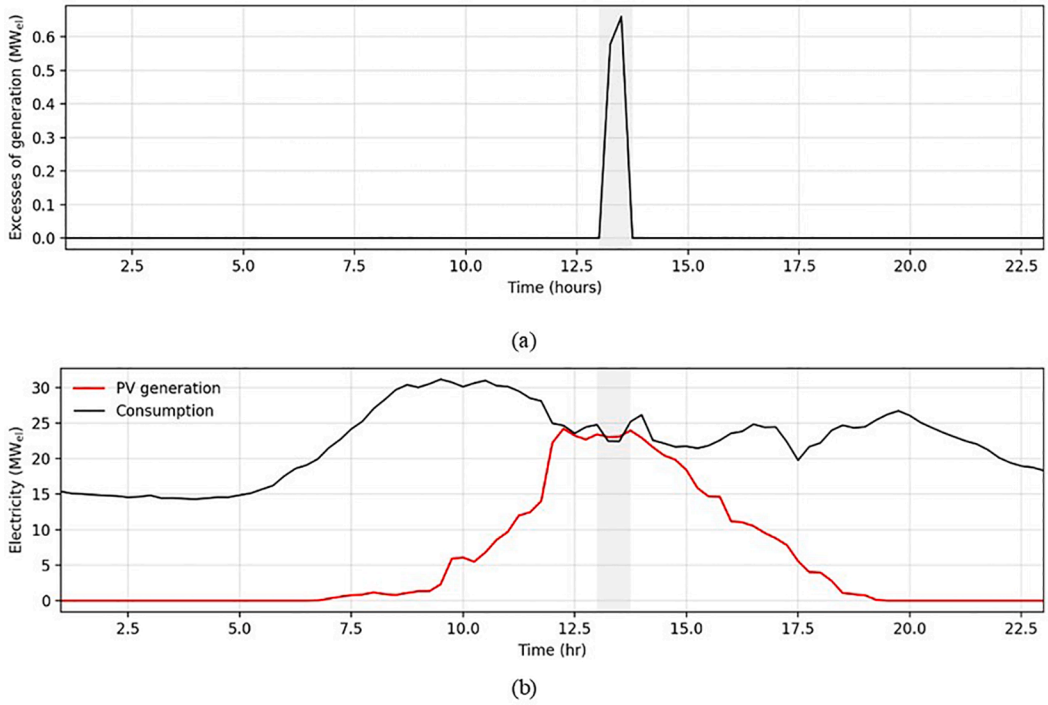

Fig. 20. (a) Excess of PV electricity production reinjected into the national grid and (b) Comparison between PV generation and electricity demand. (4 April 2018).

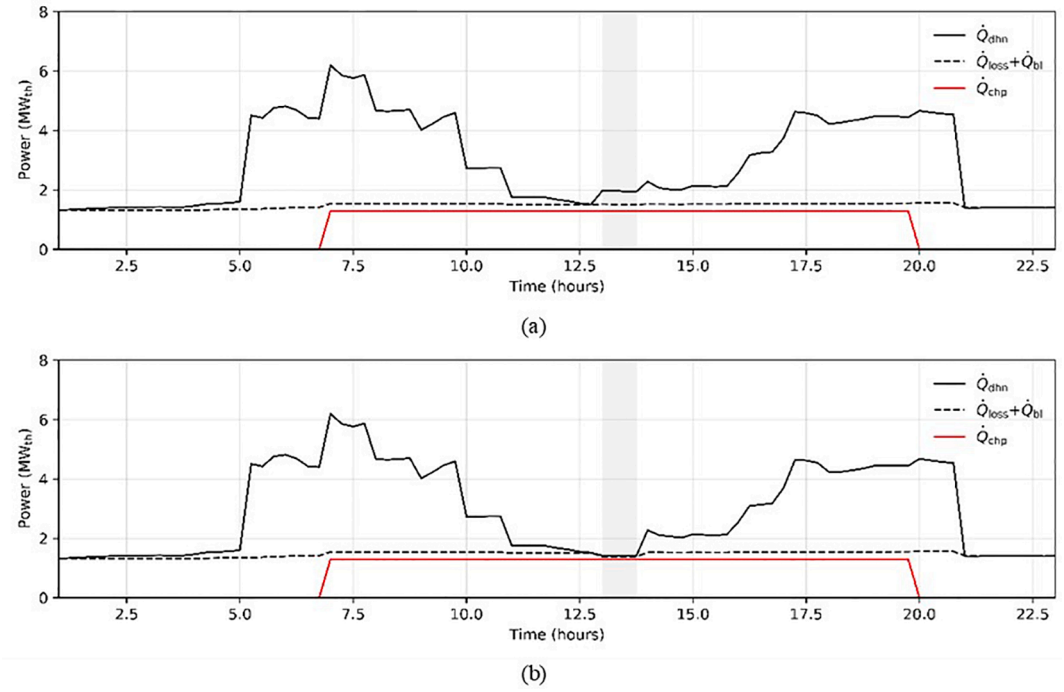

Fig. 21. Total thermal energy demand with distinction of the components related to CHP and baseload added to thermal losses: (a) normal operation and (b) all the space heating systems switched off between 1.00 pm and 2.00 pm. (4 April 2018).

April is selected (Fig. 20): on 4 April 2018 the excess photovoltaic production for the entire city of Osimo is comparable to the electricity production of the CHP: there is an excess of generation of 0.66 MW_e between 1.00 pm and 2.00 pm.

In Fig. 21a the breakdown of the thermal energy demand in normal operation can be seen. Fig. 21b, instead, shows the modification of the thermal energy demand when in the time span 1.00 pm-2.00 pm all the space heating systems are switched off. It is evident that the incidence of the space heating demand compared to the total energy demand is so limited, that the partial load operation of the CHP is not reached, not even in this configuration. The energy demand in the considered hour is reduced by about 15%, however it has an impact only on the boilers production, even if an extreme case with space heating completely off has been considered. Therefore, the effect of a reduction of the internal temperature setpoint would be even more limited. For example, if the internal setpoint is lowered from 20 °C to 19 °C between 7.00 and 8.00

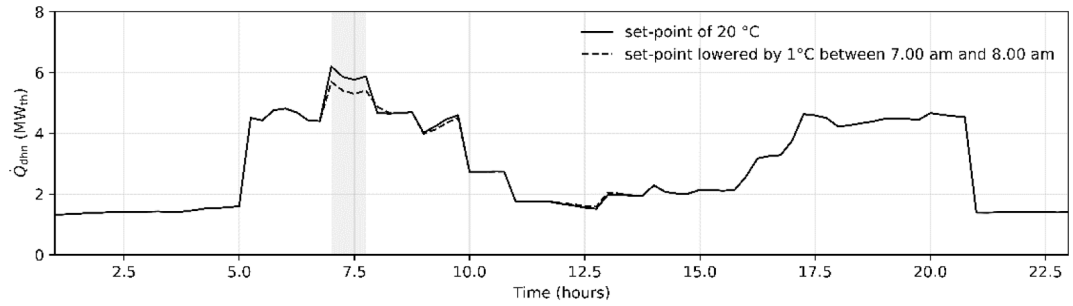

(a)

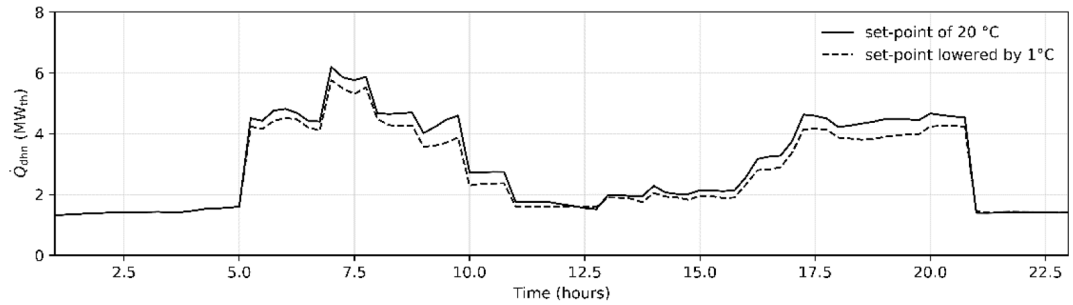

(b)

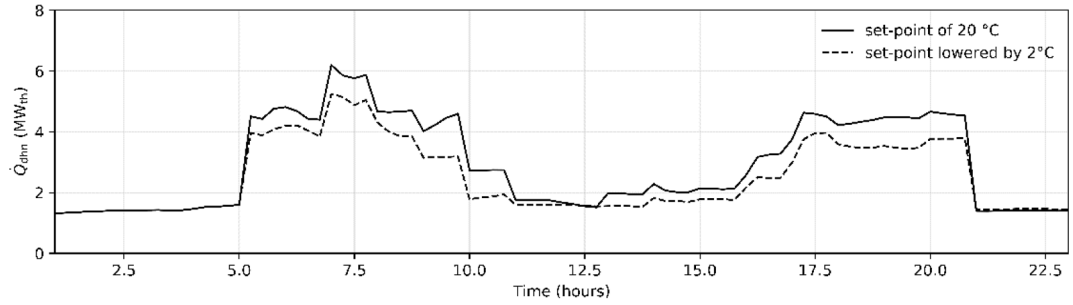

(c)

Fig. 22. (a) 1 °C reduction of the internal setpoint during the peak hour, (b) 1 °C reduction of the internal setpoint during all day and (c) 2 °C reduction of the internal setpoint during all day. (4 April 2018).

am (the peak hour), the thermal demand would decrease by about 8% in that hour.

Concluding, the internal temperature setpoints have an impact on the reduction of the total thermal demand, but the possibility of using this flexibility in the plant in Osimo for a better management of the CHP has a limited effect. However, the engagement of the end users in the energy management strategies, for example for energy conservation purposes, is very relevant. It is demonstrated by showing, for the same day considered in the previous analysis, the impact of 1 °C reduction of the internal temperature setpoint. Fig. 22 shows that by reducing of 1 °C the internal temperature setpoint during the peak hour, the daily thermal demand can be reduced by 1.5% (Fig. 22a). If the 1 °C reduction is maintained for the all-day the daily thermal demand is reduced by 7.3% (Fig. 22b) and this value can be almost doubled by means of a 2 °C temperature setpoint reduction in the same day (Fig. 22c).

7. Conclusions

The objective of this paper is to identify energy flexibility enablers in the different sections of an integrated energy system currently operating. The energy system under study is a cogeneration and district heating network (CHP-DHN) plant located in Central of Italy. Considering the constraints of the current installation, the impact of three different flexibility instruments on the energy/environmental performance are taken into account. Each of them is referred to a different part of the energy system: (i) a thermal energy storage (TES) in the generation side, (ii) an optimized control to manage the DHN supply temperature (energy distribution side) and (iii) the management of the thermostatically controlled loads (TCLs) of the final users connected to the DHN. Though the implementation of simulation models calibrated with available data, the impact of the activation of such flexibility instruments is compared with the actual operating scenario of the plant. The main results obtained can be summarized in the following points:

- The adoption of a TES coupled with the CHP-engine allows a longer operation of the CHP that can work also when the DHN demand is limited. Thanks to the presence of the TES the CHP can always run at full load, with an important increase in both thermal and electrical efficiency (increments up to 8%). The evaluation of the primary energy saving (PES) in different scenarios demonstrates this benefit. The PES increases of about 12.9% in comparison to the current operation of the CHP engine in mid-season (i.e. the CHP operates with a daily ignition program from 7.00 am to 8.00 pm), reaching the value of 19.3%. Also in the summer season it is estimated that the ignition of the CHP with the TES allows to always work the engine at full load reaching a PES of 20.6% (CHP working 24 h/24 h).
- The analysis has shown that the supply water temperature can be optimized on a daily basis taking into account the variability of the

energy demand with varying the weather conditions and it has a considerable impact on the fuel consumption of the generation plant. In a typical winter week, a 1% fuel reduction has been achieved and in a typical summer week a reduction of 2%. Extending these results to a yearly period a significant decrease in the natural gas fuel used in the plant can be produced.

- The involvement of the final users to activate the flexibility on the demand side can be effective for the specific plant, if energy conservation strategies want to be implemented. It has been assessed that 1 °C reduction of the setpoint of all the residential users during a typical winter day allows a 7.3% reduction of the DHN thermal demand. On the other hand, regarding the involvement of the final users' flexibility to influence the generation side (i.e. reduce the electricity production of the CHP at specific times when excess of renewable energy generation is available) no interesting results are obtained. However, this assessment is limited to the specific case study where the CHP engine is sized to cover the thermal baseload.

As shown by the results summarized in the three points above, all three flexibility enablers identified allow for programmed variations of the load curves of the system. Although with different effects on the energy performance of the plant, the simulations showed how a careful planning of the interventions together with the choice of a specific control strategy can increase the flexibility of the existing plant also improving its energy and environmental performance. The considerations that emerged are very much linked to the case studies analyzed, however they can provide useful hints on CHP-DHN strategies to unlock energy flexibility and could be taken as reference for other similar plants where the energy flexibility wants to be unlocked.

CRediT authorship contribution statement

A. Mugnini: Conceptualization, Methodology, Software, Validation, Writing - original draft, Formal analysis. **G. Comodi:** Conceptualization, Methodology, Writing - review & editing, Visualization, Supervision. **D. Salvi:** Methodology, Supervision, Project administration, Funding acquisition. **A. Arteconi:** Supervision, Project administration, Funding acquisition.

Declaration of Competing Interest

The authors declare that they have no known competing financial interests or personal relationships that could have appeared to influence the work reported in this paper.

Acknowledgements

This study has received funding from European Union's Horizon 2020 Research and Innovation programme under grant agreement No 824441 (MUSE GRIDS).

References

[1] E. Commission, Communication from the Commission to the European Parliament, the European Council, the Council, the European economic and social committee and the committee of the regions. The European Green Deal, (2019). eur-lex.europa.eu/legal-content/EN/TXT/?qid=1576150542719&uri=COM%3A2019%3A640%3AFIN. [accessed 22.06.2021].
[2] I.R.E.A. (IRENA), Power System Flexibility for the Energy Transition, Part 1: Overview for policy maker, (2018). www.irena.org/publications/2018/Nov/Power-system-flexibility-for-the-energy-transition. [accessed 22.06.2021].
[3] Alizadeh MI, Parsa Moghaddam M, Amjady N, Siano P, Sheikh-El-Eslami MK. Flexibility in future power systems with high renewable penetration: A review. Renew Sustain Energy Rev 2016;57:1186–119357. https://doi.org/10.1016/j.rser.2015.12.200.
[4] Gellings CW. The Smart Grid. Lilburn, GA, USA: Enabling Energy Efficiency and Demand Response; 2009.
[5] Arteconi A, Polonara F. Assessing the Demand Side Management Potential and the Energy Flexibility of Heat Pumps in Buildings. Energies. 2018;11. https://doi.org/10.3390/en11071846.
[6] Guelpa E, Marincioni L, Deputato S, Capone M, Amelio S, Pochettino E, et al. Demand side management in district heating networks: A real application. Energy. 2019;182:433–42. https://doi.org/10.1016/j.energy.2019.05.131.
[7] Sorknæs P, Østergaard PA, Thellufsen JZ, Lund H, Nielsen S, Djørup S, et al. The benefits of 4th generation district heating in a 100% renewable energy system. Energy. 2020;213:119030. https://doi.org/10.1016/j.energy.2020.119030.
[8] Cioccolanti L, Renzi M, Comodi G, Rossi M. District heating potential in the case of low-grade waste heat recovery from energy intensive industries. Appl Therm Eng 2021;191:116851. https://doi.org/10.1016/j.applthermaleng.2021.116851.
[9] Mugnini A, Coccia G, Polonara F, Arteconi A. Potential of district cooling systems: A case study on recovering cold energy from liquefied natural gas vaporization. Energies. 2019;12(15):3027. https://doi.org/10.3390/en12153027.
[10] Abokersh MH, Saikia K, Cabeza LF, Boer D, Vallès M. Flexible heat pump integration to improve sustainable transition toward 4th generation district heating. Energy Convers Manage 2020;225:113379. https://doi.org/10.1016/j.enconman.2020.113379.
[11] Badami M, Gerboni R, Portoraro A. Determination and assessment of indices for the energy performance of district heating with cogeneration plants. Energy. 2017;127:697–703. https://doi.org/10.1016/j.energy.2017.03.136.
[12] E. Commission, Directive 2012/27/EU of the European Parliament and of the Council of 25 October 2012 on energy efficiency, amending Directives 2009/125/EC and 2010/30/EU and repealing Directives 2004/8/EC and 2006/32/EC Text with EEA relevance, Volume 004 (n.d.) 202–257. data.europa.eu/eli/dir/2012/27/oj. [accessed 22.06.2021].
[13] Zhang H, Liu X, Liu Y, Duan C, Dou Z, Qin J. Energy and exergy analyses of a novel cogeneration system coupled with absorption heat pump and organic Rankine cycle based on a direct air cooling coal-fired power plant. Energy. 2021;229:120641. https://doi.org/10.1016/j.energy.2021.120641.
[14] Bogdan Ž, Damir K. Improvement of the cogeneration plant economy by using heat accumulator. Energy. 2006;31:2285–92. https://doi.org/10.1016/j.energy.2006.01.012.
[15] Shao C, Li C, You X, Wu H, Zhang J, Song Y. Optimal coordination of CHP plants with renewable energy generation considering substitutability between electricity and heat. Energy Procedia 2006;103:100–5. https://doi.org/10.1016/j.egypro.2016.11.256.
[16] Lepiksaar K, Mašatin V, Latõšov E, Siirde A, Vokova A. Improving CHP flexibility by integrating thermal energy storage and power-to-heat technologies into the energy system. Smart Energy. 2021;2:100022. https://doi.org/10.1016/j.segy.2021.100022.
[17] Vandermeulen A, van der Heijde B, Helsen L. Controlling district heating and cooling networks to unlock flexibility: A review. Energy. 2018;151:103–15. https://doi.org/10.1016/j.energy.2018.03.034.
[18] Guelpa E, Verda V. Demand response and other demand side management techniques for district heating: A review. Energy. 2021;219:119440. https://doi.org/10.1016/j.energy.2020.119440.
[19] Egging-Bratseth R, Kauko H, Knudsen BR, Bakke SA, Ettayebi A, Haufe IR. Seasonal storage and demand side management in district heating systems with demand uncertainty. Appl Energy 2021;285:116392. https://doi.org/10.1016/j.apenergy.2020.116392.
[20] Ruševljuk P, Lepiksaar K, Siirde A, Volkova A. Economic dispatch of CHP units through district heating network's demand-side management. Energies. 2021;14:4553. https://doi.org/10.3390/en14154553.
[21] Dalla Rosa A, Li H, Svendsen S. Method for optimal design of pipes for low-energy district heating, with focus on heat losses. Energy. 2011;36:2407–18. https://doi.org/10.1016/j.energy.2011.01.024.
[22] Sun F, Zhao J, Fu L, Sun J, Zhang S. New district heating system based on natural gas- fi red boilers with absorption heat exchangers. Energy. 2017;138:405–18. https://doi.org/10.1016/j.energy.2017.07.030.
[23] Chen S, Zhang G, Xia X, Setunge S, Shi L. A review of internal and external influencing factors on energy efficiency design of buildings. Energy Build 2020;216:109944. https://doi.org/10.1016/j.enbuild.2020.109944.
[24] Arteconi A, Hewitt NJ, Polonara F. State of the art of thermal storage for demand-side management. Appl Energy 2012;93:371–89. https://doi.org/10.1016/j.apenergy.2011.12.045.
[25] Verbeke S, Audenaert A. Thermal inertia in buildings: a review of impacts across climate and building use. Renew. Sustain. Energy Rev. 2020;82:2300–18. https://doi.org/10.1016/j.rser.2017.08.083.
[26] Ramos JS, Moreno MP, Delgado MG, Domínguez SÁ, Cabeza LF. Potential of energy flexible buildings: evaluation of DSM strategies using building thermal mass. Energy Build 2019;203:109442. https://doi.org/10.1016/j.enbuild.2019.109442.
[27] Stinner S, Huchtemann K, Müller D. Quantifying the operational flexibility of building energy systems with thermal energy storages. Appl Energy 2016;181:140–54. https://doi.org/10.1016/j.apenergy.2016.08.055.
[28] Arteconi A, Hewitt NJ, Polonara F. Domestic demand-side management (DSM): Role of heat pumps and thermal energy storage (TES) systems. Appl Therm Eng 2013;51:155–65. https://doi.org/10.1016/j.applthermaleng.2012.09.023.
[29] Al Essa MJM. Home energy management of thermostatically controlled loads and photovoltaic-battery systems. Energy. 2019;176:742–52. https://doi.org/10.1016/j.energy.2019.04.041.
[30] Tostado-Véliz M, Bayat M, Ghadimi AA, Jurado F. Home energy management in off-grid dwellings: Exploiting flexibility of thermostatically controlled appliances. J Cleaner Prod 2021;310:127507. https://doi.org/10.1016/j.jclepro.2021.127507.
[31] Coccia G, Mugnini A, Polonara F, Arteconi A. Artificial-neural-network-based model predictive control to exploit energy flexibility in multi-energy systems

comprising district cooling. Energy. 2021;222:119958. https://doi.org/10.1016/j.energy.2021.119958.
[32] Comodi G, Lorenzetti M, Salvi D, Arteconi A. Criticalities of district heating in Southern Europe: Lesson learned from a CHP-DH in Central Italy. Appl Therm Eng 2017;112:649–59. https://doi.org/10.1016/j.applthermaleng.2016.09.149.
[33] Python documentation, pyOpt. www.pyopt.org/reference/optimizers.slsqp.html. [accessed 22.06.2021].
[34] Mathworks, Curve Fitting. www.mathworks.com/help/curvefit/curve-fitting.html. [accessed 22.06.2021].
[35] Cadau N, De Lorenzi A, Gambarotta A, Morini M, Rossi M. Development and Analysis of a Multi-Node Dynamic. Energies. 2019;12(22):4275. https://doi.org/10.3390/en12224275.
[36] LOGSTOR, Documentation product catalogue. www.logstor.com/district-heating/cases/himmelevdenmark. [accessed 22.06.2021].
[37] TRNSYS, TRNSYS 17 Documentation, Univ. Wisconsin-Madison. (2012).
[38] UNI EN ISO, UNI EN ISO 12241: 2009. Thermal insulation for building equipment and industrial installations - calculation rules, (2009).
[39] E. Commission, Commission delegated regulation (EU) 2015/2402 of 12 October 2015 reviewing harmonised efficiency reference values for separate production of electricity and heat in application of Directive 2012/27/EU of the European Parliament and of the Council and rep, Off. J. Eur. Union. 333 (2015) 1–8. https://eur-lex.europa.eu/eli/reg_del/2015/2402/oj. [accessed 30.08.2021].